A Series of Potent and Selective, Triazolylphenyl-Based Histone Deacetylases Inhibitors with Activity against Pancreatic Cancer Cells and *Plasmodium falciparum*

Yufeng Chen,[†] Miriam Lopez-Sanchez,[§] Doris N. Savoy,[‡] Daniel D. Billadeau,[‡] Geoffrey S. Dow,[§] and Alan P. Kozikowski*[,†]

Drug Discovery Program, Department of Medicinal Chemistry and Pharmacognosy, University of Illinois at Chicago, 833 South Wood Street, Chicago, Illinois 60612, Division of Experimental Therapeutics, Walter Reed Army Institute of Research, 503 Robert Grant Avenue, Silver Springs, Maryland 20910, and Department of Immunology, Division of Oncology Research, Mayo Clinic College of Medicine, 13-42 Guggenheim, 200 First Street SW, Rochester, Minnesota 55905

Received December 20, 2007

The discovery of the rules governing the inhibition of the various HDAC isoforms is likely to be key to identifying improved therapeutics that act as epigenetic modulators of gene transcription. Herein we present results on the modification of the CAP region of a set of triazolylphenyl-based HDACIs, and show that the nature of substitution on the phenyl ring plays a role in their selectivity for HDAC1 versus HDAC6, with low to moderate selectivity (2−51-fold) being achieved. In light of the valuable selectivity and potency that were identified for the triazolylphenyl ligand **6b** in the inhibition of HDAC6 (IC_{50} = 1.9 nM), this compound represents a valuable research tool and a candidate for further chemical modifications. Lastly, these new HDACIs were studied for both their anticancer and antimalarial activity, which serve to validate the superior activity of the HDACI **10c.**

Introduction

Acetylation and deacetylation of histones play an important role in transcription regulation of eukaryotic cells.[1] The steady state of histone acetylation is established by the dynamic equilibrium between competing histone deacetylases (HDACs) and histone acetyltransferases (HATs). HATs add acetyl groups to lysine residues, while HDACs remove the acetyl groups. In general, hyperacetylation of histones facilitates gene expression, whereas histone deacetylation is correlated with transcriptional repression. The HDACs are able to control histone deacetylation, which consequently promotes chromatin condensation. HDAC[a] inhibitors (HDACIs) selectively alter gene transcription, in part, by permitting chromatin remodeling and by changing the composition of multiprotein complexes bound to proximal region of specific gene promoter.[2] Further, the HDACs interact with many nonhistone protein−substrates such as the hormone receptors, chaperone proteins, and cytoskeletal proteins, which regulate cell proliferation and cell death.[3,4]

In mammalian cells, the HDACs are divided into four classes that depend on their sequence/structural homology to yeast deacetylases, expression patterns, and catalytic mechanisms.[5,6] Eighteen HDAC enzymes have been identified and classified[3,7] based on homology to these yeast HDACs. Class I HDACs include HDAC1, 2, 3, and 8, which are related to yeast RPD3 deacetylase and they share high homology in their catalytic sites. Recent phylogenetic analyses suggest that this class can be divided into classes Ia (HDAC1 and 2), Ib (HDAC3), and Ic (HDAC8). The class II HDACs are related to yeast Hda1 (histone deacetylase 1) and include HDAC4, 5, 6, 7, 9, and 10.[8] This class is divided into class IIa, consisting of HDAC4, 5, 7, and 9, and class IIb, consisting of HDAC6 and 10, which contain two catalytic sites. All class I and II HDACs are zinc-dependent enzymes. The active site of class I and II HDACs is found within a highly conserved catalytic domain containing a divalent zinc cation that is coordinated by both histidine and aspartate residues. Deacetylation of the HDAC substrates occurs through attack by a water molecule that is activated through interaction with this zinc cation coupled with deprotonation through a histidine−aspartate charge-relay system.[9] Class III HDACs (SIRT1−7) require NAD^+ for their enzymatic activity.[10] Class IV HDAC is represented by HDAC11, which contains conserved residues in the catalytic core region shared by both class I and II enzymes.[11]

The HDACIs currently in clinical trials and preclinical development include pan-HDAC inhibitors (SAHA, **1a** and **1b**) as well as those compounds showing some level of isozyme selectivity (**1c**, **1d**, **1e**, and **1f** (Apicidin)) in Chart 1.[12] With the approval of SAHA by the FDA for the treatment of cutaneous T-cell lymphoma (CTCL) and with the ongoing evaluation of HDACIs for various cancers,[13–15] considerable interest has been growing in the application of HDACIs to a broader range of disease states, where chromatin remodeling may play a role in the pathophysiology. An important question that still needs to be adequately addressed concerns identification of the individual HDAC or subset of HDACs that one might best inhibit in order to achieve a desirable therapeutic outcome. Genetic studies, knockout studies in yeast, and the use of siRNAs in mammalian cells suggest that the class I HDACs are essential to cell proliferation and survival.[16,17] However, no conclusive experimental evidence pointed to specific HDACs as being selectively involved in cancer and other diseases.[4] Furthermore, many of the HDACIs are cytotoxic agents and induce cell-cycle arrest and apoptosis, which would, of course, prevent their use in long-term therapy. Thus difficulties may be anticipated in the application of this compound class to inflammatory diseases, malaria, psychiatric disorders, and neurodegenerative diseases. Moreover, it is not entirely clear how

* To whom correspondence should be addressed. Phone: 312-996-7577. Fax: 312-996-7107. E-mail:kozikowa@uic.edu.
[†] University of Illinois at Chicago.
[‡] Mayo Clinic College of Medicine.
[§] Walter Reed Army Institute of Research.

[a] Abbreviations: HDAC, histone deacetylase; HDACI, histone deacetylase inhibitor; HAT, histone acetyltransferase; ZBG, zinc binding group; SAHA, suberoylanilide hydroxamic acid; TSA, trichostatin A; CTCL, cutaneous T-cell lymphoma; HDLP, HDAC-like protein; HDAH, HDAC-like amidohydrolase; NOC, nitrile oxide cycloaddition; R_f, retention factor; TLC, thin-layer chromatography; MTT, 3-[4,5-dimethylthiazol-2-yl]2,5-diphenyltetrazolium bromide; HMEC, human microvascular endothelial cell.

10.1021/jm701606b CCC: $40.75
Published on Web 05/22/2008

Chart 1. Examples of HDAC Inhibitors

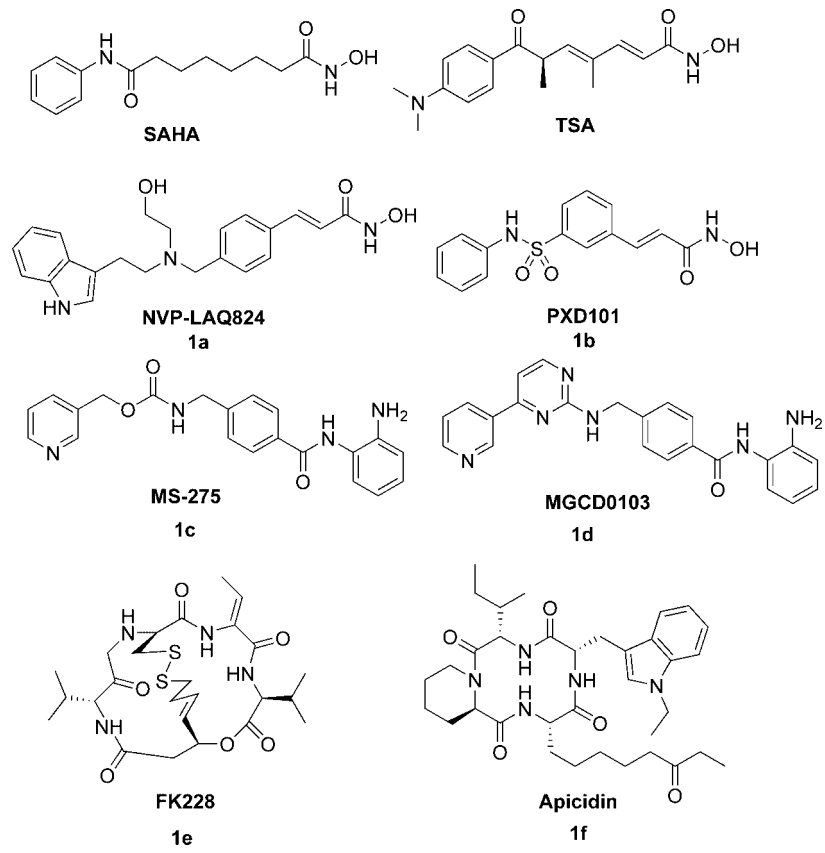

the HADCIs are working in vivo and whether histone or nonhistone-mediated effects are the most important. The development of inhibitors selective for the individual HDAC isozymes and/or conditional knockout mice may resolve some of the issues in this area.

Most HDAC inhibitors such as TSA and SAHA closely resemble the aliphatic acetyl-lysine substrate [the so-called acetylated histone tail] and deliver a hydroxamic acid or other zinc binding group to the catalytic zinc ion at the bottom of a narrow, active site pocket as seen from the cocrystal structures of inhibited HDLP (HDAC-like protein from A. aeolicus),[9] HDAH (HDAC-like amidohydrolase),[18] and the human HDAC7 (PDB: 2PQO and 2PQP) and HDAC8 (PDB: 1VKG, 1T67, 1T64, 1T69, and 2V5X).[19,20] These inhibitors all have the zinc binding group and a CAP group connected to one another through a linker comprised of a straight alkyl chain, or some modification thereof that incorporates heteroatoms, olefinic, aryl, or heteroaryl groups. Attempts to generate isozyme-specific HDAC inhibitors generally focus on varying the CAP groups to exploit the variability in the HDAC surface surrounding the active site.[21] Despite much effort, truly selective compounds are few in number, and the precise structural determinants required to achieve the selective inhibition of single HDAC isozymes generally remain undefined. To date, we have made concerted efforts to create structurally novel HDACIs with the intent to elucidate the structural parameters relevant to achieving isoform selectivity. Moreover, our plan was to study these new compounds in parallel for their therapeutic potential in cancer, stress-induced neuronal injury, and protozoan parasitic diseases. To accomplish these objectives, we chose to systematically study modifications of the CAP, linker, and zinc binding groups in order to fine-tune for isoform selectivity. Along these lines, we have shown previously that certain mercaptoacetamide-based HDACIs show inherent selectivity for HDAC6 versus HDAC1, and we have suggested that such compounds may prove valuable in the treatment of certain CNS disorders.[22] We have also suggested that certain polar or hydrophobic interactions between the CAP recognition groups and the HDAC protein surface may contribute to discrimination among the isoforms.[23] In this paper, we present our results obtained from the study of a number of triazole-based CAP groups constructed by use of the Huisgen's versatile 1,3-dipolar cycloaddition chemistry.[24,25] The present study identifies the geometric pattern of substitution in the CAP group as a possible structural determinant in achieving selectivity for HDAC6 over HDAC1. These newly synthesized ligands were screened against a panel of pancreatic cell lines and *Plasmodium falciparum* strains, and these data are presented as well.

Results and Discussion

Chemistry. The synthesis of the triazole-based ligands **6a**−**6d**, **10a**−**10d**, **12a**−**12d**, and **14a**−**14d** was accomplished according to the synthetic protocols shown in Schemes 1 and 2. The 1,3-dipolar cycloaddition reaction ("click-chemistry") of an azide with an alkyne catalyzed by a copper (I) salt[26,27] or by $Cp^*RuCl(PPh_3)_2$[28] has recently been reported to generate either a 1,4-disubstituted or a 1,5-disubstituted triazole, regioselectively. This dipolar cycloaddition chemistry, much like our previously reported applications of the nitrile oxide cycloaddition (NOC) reaction,[29] provides efficient and complementary synthetic strategies to assemble diverse templates aimed at the discovery and optimization of lead compounds. At the beginning of this research, we first synthesized ligand **6a** and screened it against a panel of HDAC isoforms. The selectivity measured for this ligand for HDAC6 versus HDAC1 (>20-fold) appeared to be promising when compared with the pan-inhibition shown

Scheme 1. Synthesis of 1,4-Disubstituted Triazole Ligands **6a**−**6d** and **10a**−**10d**[a]

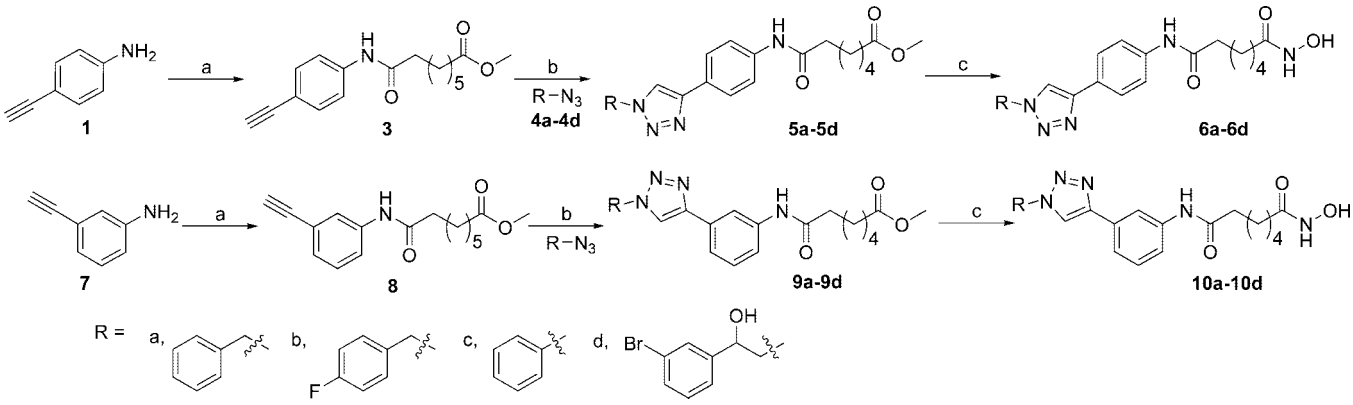

[a] Reagents and conditions: (a) Suberic acid monomethyl ester, $POCl_3$, pyridine, 0 °C; (b) copper (II) sulfate pentahydrate, sodium ascorbate, azide **4a-4d**, rt; (c) NH_2OH, KOH, rt.

Scheme 2. Synthesis of 1,3-Disubstituted Triazole Ligands **12a**−**12d** and **14a**−**14d**[a]

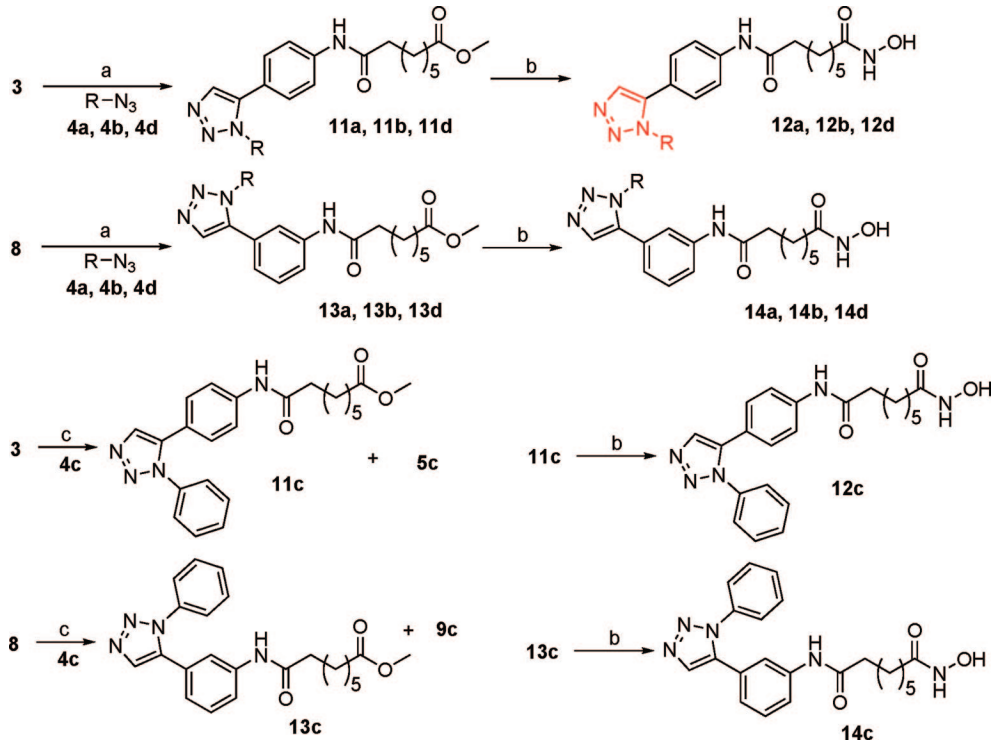

[a] Reagents and conditions: (a) Cp*$RuCl(PPh_3)_2$, azide **4a**, **4b**, and **4d**, THF, reflux; (b) NH_2OH, KOH, rt; (c) **4c**, toluene, reflux.

by SAHA (Table 1) Thus, we chose to expand upon this lead scaffold possessing the triazole core in order to characterize the structural determinants relevant to achieving higher levels of isoform selectivity. Three azides were chosen for the first round of optimization of ligand **6a**, and modifications were made to probe functional group tolerability on the terminal phenyl ring (**6b**), presence of a spacer between the terminal phenyl ring and the triazole ring (**6c**), and presence of an additional hydrogen bond donor (**6d**). Moreover, the regioisomeric triazoles **10a**−**10d** were prepared from the meta-substituted aniline **7** in order to examine the effects of geometry on isoform selectivity. As shown in Scheme 1, the $POCl_3$-pyridine-mediated coupling of suberic acid monomethyl ester with 4-ethynylaniline (**1**) yielded amide **3**, which underwent cycloaddition with azide **4a** catalyzed by $CuSO_4$ and sodium ascorbate[30] to give the 1,4-disubstituted triazole **5a** in good yield and regioselectivity. Displacement of the methyl ester moiety in **5a** by hydroxylamine afforded the final hydroxamic acid **6a**. Following a similar sequence of reactions, ligands **6b**−**6d** and **10a**−**10d** were prepared in good yield.

Scheme 2 outlines the synthesis of the 1,5-disubstituted triazoles (**12a**−**12d** and **14a**−**14d**). The 1,3-Dipolar cycloaddition between **3** and **4a** was carried out in refluxing THF under argon to afford the 1,5-disubstituted triazole **11a** regioselectively. This intermediate was subsequently converted to the hydroxamic acid **12a** using the same conditions as described above. Hydroxamic acids **12b** and **12d** were synthesized readily using the same reaction conditions. However, the synthesis of hydroxamic acids **12c** and **14c** from phenylazide **4c** and the acetylene **3** or **8** with ruthenium catalyst failed to provide the desired products, even after prolonged reaction times at higher temperatures. Finally, we switched to the standard Huisgen reaction conditions. Thus, on heating an excess of the phenylazide and acetylene **3** in refluxing toluene for 2 days, we

Table 1. HDAC Isoform in Vitro Inhibition Profiles for Prepared Triazole Ligands

		IC_{50} (nM) values against HDAC isoforms[b]						Selectivity	
Compd	Structure	HDAC 1	HDAC 2	HDAC 3	HDAC 8	HDAC 10	HDAC 6	HDAC1/ HDAC6	HDAC1/ HDAC10
SAHA[a]	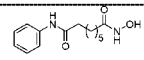	68	164	48	1524	NA	90	0.8	-
TSA	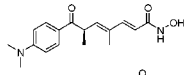	4	14	2	1380	5	1	4	0.8
6a	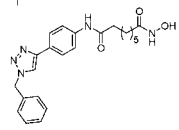	113 ± 10	679 ± 62	ND[c]	3970 ± 190	188 ± 31	4.8 ± 0.3	24	0.6
6b	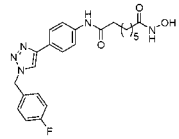	97.8 ± 16.0	294 ± 34	13.7 ± 0.4	797 ± 39	112 ± 21	1.9 ± 0.1	51	0.9
6c	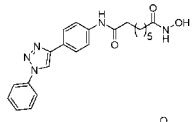	27.1 ± 2.0	47.5 ± 1.8	8.0 ± 0.3	1970 ± 180	36.1 ± 1.7	1.3 ± 0.1	21	0.8
6d	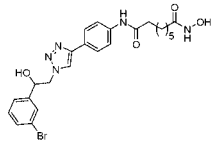	69.2 ± 3.5	143 ± 4	25.3 ± 0.8	3130 ± 200	86.5 ± 1.2	4.4 ± 0.2	16	0.8
10a	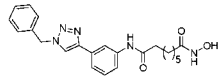	14.5 ± 1.8	43 ± 3	7.9 ± 0.3	1990 ± 120	18.5 ± 3.8	3.1 ± 0.2	5	0.8
10b	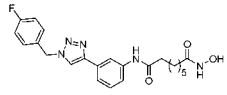	17.6 ± 0.7	77.4 ± 7.1	4.0 ± 0.2	552 ± 93	34.3 ± 7.8	2.6 ± 0.2	7	0.5
10c	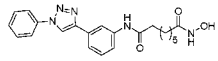	18 ± 2	63.9 ± 12.5	7.2 ± 0.7	2780 ± 470	27.7 ± 1.9	9.6 ± 0.6	2	0.6
10d	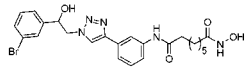	14.9 ± 1.8	64.4 ± 4.4	2.7 ± 0.1	440 ± 38	13 ± 1	1.9 ± 0.1	8	1.1
12a	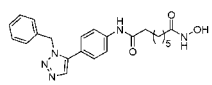	68.3 ± 7.9	124 ± 5	9.7 ± 0.5	790 ± 83	70.1 ± 6.2	3.1 ± 0.2	22	1.0
12b	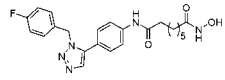	52.4 ± 1.7	57.4 ± 1.8	16.4 ± 0.9	2010 ± 120	64.7 ± 2.5	7.3 ± 0.4	7	0.8
12c	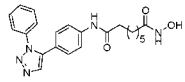	70.5 ± 3.9	146 ± 10	12 ± 1	518 ± 26	55.7 ± 4.3	3.5 ± 0.0	20	1.3
12d	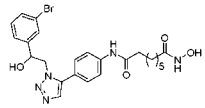	69.9 ± 10.1	216 ± 19	15.1 ± 0.8	737 ± 40	74.8 ± 8.6	4.2 ± 0.2	17	0.9
14a	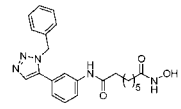	18.6 ± 1.9	112 ± 12	4.5 ± 0.5	433 ± 26	19.2 ± 1.4	3.3 ± 0.3	6	1.0
14b	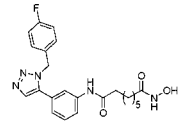	25.9 ± 4.5	124 ± 8	5.8 ± 0.2	529 ± 39	17.6 ± 2.3	3.8 ± 0.1	7	1.5
14c	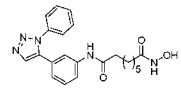	33.4 ± 2.0	167 ± 11	7.7 ± 0.3	942 ± 67	24.5 ± 2.4	7.5 ± 0.2	4	1.4
14d	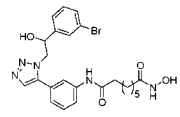	23.4 ± 4.0	116 ± 9	4.2 ± 0.4	406 ± 21	15.8 ± 2.3	2.8 ± 0.3	8	1.5

[a] Taken from reference 32. [b] The isoform inhibition was tested at Amphora Discovery Corporation (http://www.amphoracorp.com/). [c] Not determined.

Chart 2. Compound **6a** and Tubacin

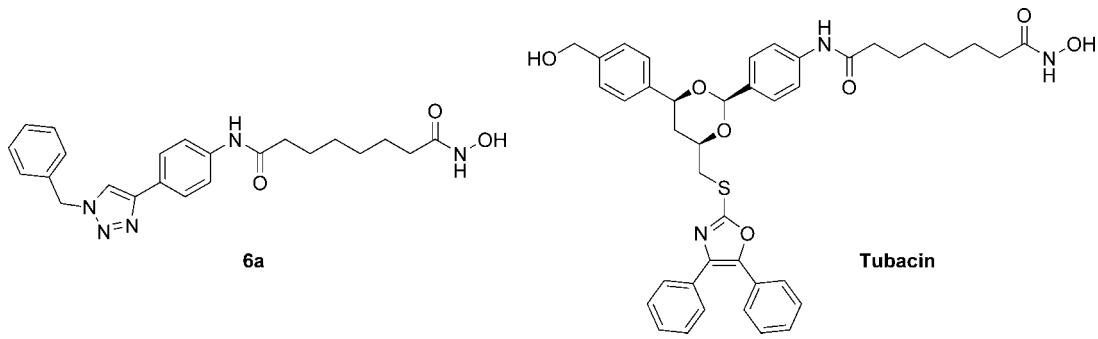

obtained the 1,4- and 1,5- disubstituted triazoles **5c** and **11c**. The same reaction of the phenylazide and acetylene **8** resulted in 1,4- and 1,5- disubstituted triazoles **9c** and **13c**. Structures of **11c** and **13c** have been elucidated based upon comparison of retention factor (R_f) on thin-layer chromatography (TLC) and the NMRs between **11c** vs **5c** and **13c** vs **9c**, which were obtained from the copper catalyzed cycloaddition reactions in Scheme 1. Treatment of **11c** and **13c** with hydroxylamine and KOH gave the corresponding hydroxamic acids **12c** and **14c**.

HDAC Isoform Inhibition Assay. The new HDACIs described above were screened both in vitro for enzyme-inhibitory activity and then for their ability to block cancer cell growth and *P. falciparum* growth. The inhibitory effects of these compounds on histone deacetylase (HDAC) activity were determined using a fluorescence-based assay with electrophoretic separation of substrate and product carried out using a microfluidic system followed by quantitation of fluorescence intensity in the substrate and product peaks. The assays were performed using isolated HDAC isoforms that had been expressed as 6× His-tagged fusion proteins in a baculovirus expression system in Sf9 cells. HDACs 1, 2, 3, 6, and 8 were expressed as full length fusion proteins. The HDAC10 fusion protein was expressed as a carboxy-terminal deletion of 38 amino acids (residues 632−669). HDAC3 was coexpressed with a fragment of the SMRT gene (residues 395−489) to generate enzymatically active protein. The data are presented as IC_{50} values in Table 1. TSA was used as a positive control. The recently published inhibitory data for SAHA against a panel of recombinant HDACs are also presented for comparison.

Results and Discussion

The results of the HDAC isoform assays are shown in Table 1. As noted above, the present study evolved as a consequence of our finding that compound **6a** showed some degree of selectivity for HDAC6 versus HDAC1. Compared to other members of this zinc-dependent HDAC family, HDAC6 deacetylates tubulin[31] and HSP90.[32] HDAC6 has a specific ubiquitin-binding domain at the C-terminus that associates with protein ubiquitination and inhibition of proteasome.[33] Recently, HDAC6 was shown to be required for the autophagic degradation of aggregated mutant HTT in mouse neuroblastoma cells owing to its function in the transportation of autophagosomes and lysosomes.[34] Tubacin, a specific inhibitor of HDAC6 that inhibits the deacetylation of α-tubulin but not of histones,[35–37] and RNA interference techniques have been used as research tools in elucidating the cellular function of HDAC6 and its substrates. Because of the important role of HDAC6 in human biology, more selective small molecule inhibitors of HDAC6 or even substrate-selective HDAC6 inhibitors are in great demand. Recently a new class of thiol- and lysine-based HDAC6 selective inhibitors has been identified, and in this class of ligands, the selectivity between deacetylation of histone H4 and α-tubulin could be modified by varying the CAP region functional groups.[38,39] In the present research, the newly identified HDAC6 selective ligand **6a** shares the same linker and zinc binding group as found in tubacin, which was identified through combinatorial synthesis and cell-based screening of a >7000-compound library.[21] The structural differences between tubacin and **6a** are easily discerned. Tubacin structure is a T-shaped molecule, while **6a** is a linear molecule (Chart 2).

Consistent with the isoform inhibitory profile of **6a**, the *p*-fluorinated compound **6b** shows even better selectivity for HDAC6 over HDAC1 (51-fold). For compounds **6c** and **6d**, the inhibition of HDAC1 increased slightly, but the selectivity between HDAC6 and HDAC1 is similar to that of **6a** (21-fold for **6c** and 16-fold for **7d**). On the other hand, a decreased level of selectivity between HDAC6 and HDAC1 was found for ligands **10a**−**10d** (2−8-fold). Within this small library, ligand **10c** shows the lowest level of selectivity between HDAC6 and HDAC1 (only 2-fold). It is apparent that this subclass of ligands **10a**−**10d** shows better HDAC1 inhibition than their regioisomers **6a**−**6d**, thus accounting for their lower selectivity index. On the basis of the SAR shown here, it is likely that further levels of HDAC6 selectivity could be achieved through further modifications of the terminal phenyl ring of **6a** and **6b.**

A similar but slightly decreased level of selectivity variation in the inhibition of HDAC1 versus HDAC6 was found by the compounds belonging to the two subclasses of 1,5-disubstituted triazoles, namely **12a**−**12d** and **14a**−**14d** (7−22-fold versus 4−8-fold). In general, structural variations in the triazole ring functionality do not play a significant role in the selectivity for inhibition of HDAC6 over HDAC1 compared with the substitution pattern of the central phenyl ring (para versus meta). This finding may be a consequence of the location of the central phenyl group nearer to the entrance of the enzyme's catalytic pocket.[9,19,20] Consistent with our previous paper concerning *p*-substituted biphenyl bearing HDAC inhibitors,[23] as well as the tubacin-like molecules,[35–37] this 1,4-substituted phenyl CAP might thus contribute to the preferable inhibition of HDAC6 over HDAC1, although further chemistry biology studies will be needed to confirm this hypothesis.

In addition to the subclass selectivity for HDAC6 versus HDAC1, minor changes in structure and geometrical orientation of the CAP region recognition groups was found to lead to differences in inhibitory activity against some of the other isozymes. For example, the benzyl triazole **6a** is more than 10-fold less active in inhibiting HDAC2 compared to its phenyl counterpart **6c** (IC_{50}: 47.5 nM for **6c** and 679 nM for **6a**). The inhibition of HDAC10 by **10a** increases almost 10-fold compared with that of its regioisomer **6a** (IC_{50}: 18.5 nM for **10a**

Table 2. In Vitro Inhibition against Pancreatic Cancer Cell Lines by the Triazole-Based HDAC Inhibitors

	inhibition of pancreatic cancer cell lines (IC_{50}, μM)				
compd	BxPC-3	Hup T3	Mia Paca-2	Panc 04.03	SU 86.86
SAHA	5	0.8	1.1	1.2	1.3
6a	9	5	<1	2	10
6b	22	4	<0.5	3	11
6c	3	1	0.4	1	1
6d	18	12	0.6	10	12
10a	3	1	<0.5	2	2
10b	1	1	0.3	1	1
10c	0.4	0.2	0.02	<0.5	0.8
10d	11	11	0.8	14	12
12a	11	5	2	2	9
12b	11	4	8	2	10
12c	13	10	8	8	11
12d	25	46	37	44	42
14a	12	2	1	4	7
14b	11	5	2	9	8
14c	10	8	3	2	4
14d	43	42	11	25	23

Table 3. In Vitro Inhibition against Nontransformed Human Cells by the Triazole-Based HDAC Inhibitors

	inhibition of nontransformed cells (IC_{50}, μM)	
compd	HMEC	HPDE6c7
SAHA	1.3	1.3
6c	1	1
10b	<1	0.5
10c	<1	<0.2

and 188 nM for **6a**). In general, the selectivity of these inhibitors for HDAC1 and HDAC10 vary less than the selectivity measured between HDAC1 and HDAC6. The majority of these compounds fail to provide any remarkable levels of isoform selectivity, and all of them show only weak activity for HDAC8.

Although the present findings are of interest and can be analyzed in a number of ways, it is well appreciated that the isozyme selectivity shown by an HDACI can vary within the context of the whole cell in light of the fact that, inter alia, the HDACs form complexes involving both other HDACs as well as corepressor proteins (e.g., mSin3A−HDAC complex). Moreover, some of these HDACs may work together in a complementary fashion, whereas others may oppose one another in terms of their ultimate effects on gene transcription. As such, both cell-based screening methods and diverse disease models together with appropriate ADMET studies remain relevant to evaluating the true value of any new HDACIs. Below we present the preliminary results of both the growth inhibition of these triazole-based HDACIs against a panel of pancreatic cancer lines, nontransformed cells, and *P. falciparum* strains (Tables 2, 3, and 4).

Pancreatic Cancer Lines Proliferation Assay. Pancreatic cancer is the fourth leading cause of cancer death in the United States and essentially remains an incurable disease with a five-year survival of less than 5%. There is increasing evidence that signaling and transcriptional pathways that control cell proliferation, differentiation, and apoptosis are dysregulated in pancreatic cancer. Recently, SAHA had been tested against six pancreatic cancer cell lines and showed induction of apoptosis, G2 cell cycle arrest, and differentiation. Also, the combination of SAHA and an inhibitor of DNA methylation, 5-aza-2′-deoxycytidine, had an enhanced antiproliferative effect toward pancreatic cancer cells.[40] At present, there exists no effective therapy against pancreatic cancer.

Table 4. In Vitro Growth Inhibition of *P. falciparum* Strains by the Triazole-Based HDAC Inhibitors

	inhibition of *P. falciparum* (IC_{50}, nM)			
compd	D6	W2	TM90C235	TM90C2A
chloroquine[a]	14 ± 6	405 ± 206	138 ± 71	189 ± 46
mefloquine[a]	11 ± 5.6	5.9 ± 2.1	42 ± 23	46 ± 22
SAHA	247	161	310	110
6a	210	530	300	160
6d	80	390	110	190
10a	140	160	220	190
10b	180	350	280	110
10c[b]	17 [17−18]	32 [20−45]	35 [31−39]	17 [15−19]
10d	110	560	260	110
12a	400	>1200	520	300
12b	240	460	290	120
12c	350	620	470	170
12d	230	>950	390	230
14a	210	600	370	150
14b	300	590	460	210
14c	320	730	500	330
14d	180	380	390	120

[a] Data represent average IC_{50} +/− STDEV for last 20 assays. [b] Values represent mean of two experiments with range in brackets.

In the development of HDAC inhibitors as anticancer therapeutics, it will be invaluable to elucidate the interplay of the structural parameters relevant to isoform inhibitory activity, antiproliferative activity, and toxicity to normal cells. It is still unclear, for example, as to whether pan-selective HDACIs, such as SAHA and **1b**, are superior to class I selective inhibitors such as **1c** and **1d**.[41] In this work, these new triazole-based ligands were tested for their antiproliferative activity against a panel of pancreatic cancer cell lines, which consisted of BxPC-3, Hup T3, Mia Paca-2, Pan 04.03, and SU 86.86 cells. Cell growth inhibition of the tested analogues was measured by MTT assay, and the IC_{50} values obtained against these cell lines are summarized in Table 2. Comparison data are provided for SAHA. All compounds in this library demonstrated reasonably good antiproliferative activity against all cancer cell types examined, especially for the Mia Paca-2 line. This finding is consistent with an earlier report showing that the cyclopeptide-based HDAC inhibitor **1e** was most active against Mia Paca-2 when tested against a panel of five pancreatic cancer lines.[42] In our triazole library, **10c** gave the best inhibition against all pancreatic cancer cell lines, with the lowest IC_{50} value being shown against the Mia Paca-2 cell (20 nM). For comparison we note that the structurally related regioisomers **6c**, **12c**, and **14c** showed different inhibitory profiles. In general, the 1,4-disubstituted triazoles showed better cell inhibitory activity than the 1,5-disubstituted triazoles. Another trend from this small library of compounds is that the meta-substituted phenyl ring compounds **10a**−**10d** are more potent than their para-substituted counterparts **6a**−**6d**. The previous experience on the biphenyl-based HDAC inhibitors indicated that the meta-substituted biphenyl HDACIs were more potent in cellular assays than the *p*-biphenyl counterparts.[43] But this trend is not obvious in the subclass of vicinal disubstituted triazole ligands **12a**−**12d** and **14a**−**14d**. It is valuable to note that the subclass of ligands **10a**−**10d** has the lowest selectivity between HDAC1 and HDAC6 in this library, and yet these compounds show better antiproliferative activity than their regioisomers possessing higher isozyme selectivity, **6a**−**6d**. These data may further substantiate the importance of potency in the inhibition of the nuclear HDAC1 in the induction of cancer cell apoptosis, as this particular HDAC is involved in the regulation of the c-jun promoter.[44]

We further measured the cytotoxicity the three most active ligands, **6c**, **10b**, and **10c**, against two human normal cells,

namely HMEC (human microvascular endothelial cell) and HPDE6c7 (an immortalized nontransformed pancreatic epithelial cell line), and SAHA was chosen as control (Table 3). A similar extent of inhibition was found out between the tested pancreatic cancer cells and nontransformed cells, including SAHA.

Activity against *P. falciparum*. Falciparum malaria is responsible for more than a million deaths a year, mostly in sub-Saharan Africa.[45] There is a general need to find new antimalarial drugs with novel modes of action, given that there is only one class of antimalarial drugs (artemisinin derivatives) effective against all drug-resistant malaria. Initial studies suggest that HDAC may be an attractive target in *P. falciparum*. The potential antimalarial activity of HDAC inhibitors was reported by Darkin-Rattray et al. in 1996.[46] **1f**, a fungal metabolite, was found to exhibit a minimum inhibitory concentration of 125 ng/mL against *P. falciparum* and exhibited a suppressive effect on blood-stage parasites when administered orally at a dose rate of 50 mg/kg. Functional studies suggested that the target of **1f** was indeed malarial parasite HDAC. The compound did not appear to have much selectivity for malaria because its IC_{50} against proliferating mammalian cells was 50−100 nM. Subsequently, Joshi et al. subcloned an HDAC directly from *P. falciparum*, showed that it localized in the parasite nucleus, and was expressed primarily in mature asexual blood stages and in gametocytes.[47] A subsequent study also demonstrated that other putative HDAC inhibitors were active in vitro and in vivo.[48] These studies suggest that HDAC is a promising target in malaria but have not yielded a promising lead candidate.

Some of the triazole analogs described here display interesting antimalarial activity. The 50% inhibitory concentrations (IC_{50}s) against a number of drug resistant strains of *P. falciparum* are presented in Table 4. Most of the analogs exhibit IC_{50}s > 100 nM against all strains tested, whereas mefloquine has an IC_{50} of 5.9 nM against the sensitive W2 strain while chloroquine has an IC_{50} of 14 nM against the sensitive D6 strain. In contrast, compound **10c** is an order of magnitude more potent than most of the other compounds tested and is more active than mefloquine and chloroquine against the multiple drug-resistant strains C235 and C2A. Compound **10c** exhibits potency equivalent to TSA[48] and **1f**[47] and is more active by orders of magnitude than other HDAC inhibitors evaluated by Andrews et al.[48] The selectivity indices of compound **10c** relative to *P. falciparum* C235 were 0.62, 5.7, 11.4, and 22.8 against the Mia Paca-2, Hup T3, Bx-PC-3, and SU 86.86 cell lines, respectively. Thus, for three of the four mammalian cell lines, **10c** displayed more selectivity for *P. falciparum* than was reported for **1f**[47] in earlier studies. Consequently, it may represent a useful lead structure for the synthesis of new HDAC inhibitors with selectivity for malaria. ADME studies are ongoing in our laboratory at WRAIR to determine the viability of **10c** as a lead candidate.

Summary. The present studies further add to the ever growing database of structural information that is relevant to the design of isozyme selective HDACIs. Modification of the CAP region of the present set of triazolylphenyl-based HDACIs reveals that the nature of substitution of the phenyl ring plays a role in their selectivity for HDAC1 versus HDAC6, with low to moderate selectivity (2−51-fold) being achieved. In light of the valuable selectivity and potency shown by ligand **6b** in the inhibition of HDAC6, this compound represents a useful research tool and would appear to represent a candidate for further chemical modifications. Moreover, the anticancer and antimalarial screening studies validate the superior activity of the HDACI **10c**, however, both in vivo and ADMET studies will be required to qualify this as a real drug lead. Additionally, efforts are being made to obtain measurements of IC_{50} values against the missing HDAC isoforms, which will be reported in due course.

Experimental Section

Chemistry. ^{1}H NMR and ^{13}C NMR spectra were recorded on Bruker spectrometer at 300/400 MHz and 75/100 MHz, respectively, with TMS as an internal standard. HRMS experiment was performed on Q-TOF-2TM (Micromass). TLC was performed with Merck 60 F_{254} silica gel plates. Preparative TLC was performed with Analtech 1000 μm silica gel GF plates. Column chromatography was performed using Merck silica gel (40−60 mesh). HPLC was carried out on an ACE AQ columns (100 mm × 4.6 mm and 250 mm × 10 mm), with detection at 210, 240, 254, 280, and 300 nm on a Shimadzu SPD-10A VP detector; flow rate = 2.0−3.5 mL/min; from 10% acetonitrile in water to 100% acetonitrile with 0.05% TFA.

7-(4-Ethynylphenylcarbamoyl)heptanoic Acid Methyl Ester (3). To a solution of 4-ethynylaniline (**1**, 2.00 g, 7 mmol) and suberic acid monomethyl ester (**2**, 3.21 g, 17 mmol) in 30 mL of dry pyridine at 0 °C was added 3.14 g (21 mmol) of $POCl_3$ dropwise. This solution was stirred at this temperature for 30 min, then diluted with EtOAc and washed thoroughly with saturated aqueous $KHSO_4$ and brine, dried over Na_2SO_4, filtered, and concentrated. Silica gel chromatography (hexanes/EtOAc 3:1) of the crude mixture afforded 2.16 g (44%) of **3**. R_f = 0.35 (2:1 hexane:EtOAc). ^{1}H NMR (DMSO-d_6, 400 MHz) δ (ppm): 10.01 (s, 1H), 7.59 (d, J = 8.4 Hz, 2H), 7.38 (d, J = 8.0 Hz, 2H), 4.05 (s, 1H), 3.56 (s, 3H), 2.31−2.26 (m, 4H), 1.58−1.49 (m, 4H), 1.22 (br s, 4H). ^{13}C NMR (DMSO-d_6, 100 MHz) δ (ppm): 173.7, 171.9, 140.3, 132.7, 119.2, 116.2, 84.0, 80.1, 51.6, 36.8, 33.6, 28.7, 28.6, 25.2, 24.7.

7-[4-(1-Benzyl-1*H*-[1,2,3]triazol-4-yl)phenylcarbamoyl]heptanoic Acid Methyl Ester (5a). In a mixture of **3** (100 mg, 0.34 mmol) and benzyl azide (**4a**, 124 mg, 1.04 mmol) in water and ethyl alcohol (v/v = 1:1, 10 mL) sodium ascorbate (28 mg, 0.14 mmol, dissolved in 1 mL of water) was added, followed by the addition of copper(II) sulfate pentahydrate (18 mg, 0.07 mmol, dissolved in 1 mL of water). The heterogeneous mixture was stirred vigorously overnight at room temperature. TLC analysis indicated complete consumption of the **3** in 12 h. The reaction mixture was diluted with EtOAc and washed thoroughly with brine, dried over Na_2SO_4, filtered, and concentrated. Silica gel chromatography (hexanes/EtOAc 1:1) of the crude mixture afforded 97 mg (66%) of **5a**. R_f = 0.62 (1:2 hexane:EtOAc). ^{1}H NMR (DMSO-d_6, 400 MHz) δ (ppm): 9.93 (s, 1H), 8.52 (s, 1H), 7.75 (d, J = 7.6 Hz, 2H), 7.64 (d, J = 8.0 Hz, 2H), 7.38−7.33 (m, 5H), 5.62 (s, 2H), 3.57 (s, 3H), 2.29 (t, J = 7.2 Hz, 4H), 1.57−1.52 (m, 4H), 1.29 (br s, 4H). ^{13}C NMR (DMSO-d_6, 100 MHz) δ (ppm): 171.1, 147.0, 139.4, 136.4, 129.2, 128.5, 128.3, 126.0, 125.7, 121.3, 119.6, 53.4, 51.6, 36.7, 33.6, 28.7, 28.6, 25.3, 24.7.

7-{4-[1-(4-Fluorobenzyl)-1*H*-[1,2,3]triazol-4-yl]phenylcarbamoyl}-heptanoic Acid Methyl Ester (5b). Compound **5b** (yield 80%) was prepared according to the methodology described for the preparation of compound **5a** by substituting **4a** with 4-fluorobenzyl azide (**4b**). R_f = 0.45 (1:2 hexane:EtOAc). ^{1}H NMR (DMSO-d_6, 400 MHz) δ (ppm): 9.93 (s, 1H), 8.51 (s, 1H), 7.74 (d, J = 8.4 Hz, 2H), 7.64 (d, J = 8.4 Hz, 2H), 7.43−7.40 (m, 2H), 7.24−7.19 (m, 2H), 5.61 (s, 2H), 3.56 (s, 3H), 2.29 (t, J = 6.8 Hz, 4H), 1.59−1.52 (m, 4H), 1.29 (br s, 4H). ^{13}C NMR (DMSO-d_6, 100 MHz) δ (ppm): 173.7, 171.7, 163.5, 161.1, 147.0, 139.4, 132.7, 130.7, 130.6, 126.0, 125.7, 121.2, 119.6, 116.1, 115.9, 52.6, 51.6, 36.7, 33.6, 28.7, 28.6, 25.3, 24.7.

7-[4-(1-Phenyl-1*H*-[1,2,3]triazol-4-yl)phenylcarbamoyl]heptanoic Acid Methyl Ester (5c). Compound **5c** (yield 57%) was prepared according to the methodology described for the preparation of compound **5a**, by substituting **4a** with phenyl azide (**4c**). R_f = 0.70 (1:2 hexane:EtOAc). ^{1}H NMR ($CDCl_3$, 400 MHz) δ (ppm): 8.19 (s, 1H), 7.88 (d, J = 8.4 Hz, 2H), 7.81 (d, J = 7.6 Hz, 2H), 7.66 (d, J = 8.0 Hz, 2H), 7.57 (t, J = 7.6 Hz, 1H), 7.54 (d, J = 5.6 Hz,

1H), 7.48 (d, $J = 7.6$ Hz, 1H), 7.00 (s, 1H), 3.69 (s, 3H), 2.40 (t, $J = 7.2$ Hz, 2H), 2.34 (t, $J = 7.2$ Hz, 2H), 1.77 (t, $J = 6.8$ Hz, 2H), 1.66 (t, $J = 7.2$ Hz, 2H), 1.41 (br s, 4H). ^{13}C NMR ($CDCl_3$, 100 MHz) δ (ppm): 173.8, 171.0, 151.1, 147.6, 137.8, 136.6, 135.3, 129.3, 128.3, 127.8, 126.1, 125.6, 125.1, 120.1, 119.6, 116.9, 51.1, 37.2, 33.8, 33.5, 29.9, 28.3, 24.9, 24.2, 20.7.

7-(4-Phenylcarbamoyl)heptanoic Acid Methyl Ester (5d). Compound **5d** (yield 77%) was prepared according to the methodology described for the preparation of compound **5a** by substituting **4a** with 2-azido-1-(3-bromophenyl)ethanol (**4d**). $R_f = 0.43$ (1:2 hexane: EtOAc). ^{1}H NMR (DMSO-d_6, 400 MHz) δ (ppm): 9.94 (s, 1H), 8.39 (s, 1H), 7.74 (d, $J = 8.4$ Hz, 2H), 7.66 (d, $J = 8.4$ Hz, 2H), 7.60 (s, 1H), 7.48 (d, $J = 8.0$ Hz, 1H), 7.38 (d, $J = 8.0$ Hz, 1H), 7.31 (t, $J = 7.6$ Hz, 1H), 5.99 (d, $J = 4.8$ Hz, 1H), 5.06−5.03 (m, 1H), 4.61−4.56 (m, 1H), 4.51−4.46 (m, 1H), 3.57 (s, 3H), 2.32−2.27 (m, 4H), 1.60−1.51 (m, 4H), 1.29 (br s, 4H). ^{13}C NMR (DMSO-d_6, 100 MHz) δ (ppm): 173.7, 171.6, 146.3, 145.2, 139.3, 130.8, 129.3, 126.0, 125.9, 125.6, 122.0, 121.9, 119.7, 71.1, 56.8, 51.6, 36.7, 33.6, 28.7, 28.6, 25.3, 24.7.

Octanedioic Acid [4-(1-Benzyl-1*H*-[1,2,3]triazol-4-yl)phenyl]-amide Hydroxyamide (6a). To a solution of hydroxylamine hydrochloride (2.64 g, 38 mmol) in 20 mL of MeOH, KOH (2.13 g, 38 mmol) was added at 40 °C for 10 min. The reaction mixture was cooled to 0 °C and filtered. Compound **5a** (80 mg, 0.19 mmol) was added to the filtrate followed by KOH (250 mg, 4.45 mmol) at room temperature for 30 min. The reaction mixture was extracted with EtOAc. The organic layer was washed with saturated NH_4Cl aqueous solution and brine, dried over Na_2SO4, filtered, and concentrated. The crude solid was purified by preparative HPLC to give compound **6a** (35 mg, 43%). ^{1}H NMR (DMSO-d_6, 400 MHz) δ (ppm): 10.34 (s, 1H), 9.96 (s, 1H), 8.54 (s, 1H), 7.76 (d, $J = 8.5$ Hz, 2H), 7.66 (d, $J = 8.5$ Hz, 2H), 7.42−7.34 (m, 5H), 6.38 (s, 2H), 2.30 (t, $J = 7.5$ Hz, 2H), 1.94 (t, $J = 7.3$ Hz, 2H), 1.58 (t, $J = 6.9$ Hz, 2H), 1.49 (t, $J = 6.7$ Hz, 2H), 1.27 (br s, 2H). ^{13}C NMR (DMSO-d_6, 100 MHz) δ (ppm): 171.3, 169.1, 146.6, 139.1, 136.1, 128.8, 128.2, 127.9, 125.6, 125.3, 120.9, 119.2, 53.0, 36.4, 32.3, 28.4, 25.0. ESI-HRMS calculated for $[C_{23}H_{27}N_5O_3 + H]^+$: 422.2186; found: 422.2180.

Octanedioic Acid {4-[1-(4-Fluorobenzyl)-1*H*-[1,2,3]triazol-4-yl]phenyl}amide Hydroxyamide (6b). Compound **6b** (yield 67%) was prepared according to the methodology described for the preparation of compound **6a**. ^{1}H NMR (DMSO-d_6, 400 MHz) δ (ppm): 10.33 (s, 1H), 9.96 (s, 1H), 8.66 (s, 1H), 8.53 (s, 1H), 7.75 (d, $J = 8.0$ Hz, 2H), 7.65 (d, $J = 8.4$ Hz, 2H), 7.42−7.41 (m, 2H), 7.25−7.21 (m, 2H), 5.62 (s, 2H), 2.30 (t, $J = 6.8$ Hz, 2H), 1.94 (t, $J = 7.6$ Hz, 2H), 1.58 (t, $J = 6.0$ Hz, 2H), 1.49 (br s, 2H), 1.28 (br s, 4H). ^{13}C NMR (DMSO-d_6, 100 MHz) δ (ppm): 171.3, 169.1, 163.1, 160.7, 146.6, 139.1, 132.3, 130.3, 130.2, 125.6, 125.3, 120.8, 119.3, 115.8, 115.5, 52.2, 36.4, 32.3, 28.4, 25.0. ESI-HRMS calculated for $[C_{23}H_{26}F_1N_5O_3 + H]^+$: 440.2092; found: 440.2086.

Octanedioic Acid Hydroxyamide [4-(1-Phenyl-1*H*-[1,2,3]triazol-4-yl)phenyl]amide (6c). Compound **6c** (yield 58%) was prepared according to the methodology described for the preparation of compound **6a**. ^{1}H NMR (DMSO-d_6, 400 MHz) δ (ppm): 10.35 (s, 1H), 10.02 (s, 1H), 9.21 (s, 1H), 8.67 (s, 1H), 7.94 (d, $J = 7.2$ Hz, 2H), 7.86 (d, $J = 7.6$ Hz, 2H), 7.71 (d, $J = 7.6$ Hz, 2H), 7.63 (t, $J = 7.6$ Hz, 2H), 7.51 (t, $J = 7.2$ Hz, 1H), 2.32 (t, $J = 6.4$ Hz, 2H), 1.94 (t, $J = 6.8$ Hz, 2H), 1.59 (br s, 2H), 1.49 (br s, 2H), 1.28 (br s, 4H). ^{13}C NMR (DMSO-d_6, 100 MHz) δ (ppm): 171.4, 169.1, 147.2, 139.4, 136.7, 130.0, 128.7, 125.8, 124.9, 120.0, 119.3, 118.9, 35.8, 32.3, 28.4, 25.1, 25.0. ESI-HRMS calculated for $[C_{22}H_{25}N_5O_3 + H]^+$: 408.2030; found: 408.2025.

Octanedioic Acid (4-{1-[2-(3-bromophenyl)-2-hydroxyethyl]-1*H*-[1,2,3]triazol-4-yl}phenyl)amide Hydroxyamide (6d). Compound **6d** (yield 41%) was prepared according to the methodology described for the preparation of compound **6a**. ^{1}H NMR (DMSO-d_6, 400 MHz) δ (ppm): 10.34 (s, 1H), 9.96 (s, 1H), 8.66 (s, 1H), 8.41 (s, 1H), 7.76 (d, $J = 8.5$ Hz, 2H), 7.67 (d, $J = 8.1$ Hz, 2H), 7.61 (s, 1H), 7.49 (d, $J = 8.3$ Hz, 1H), 7.40 (d, $J = 7.5$ Hz, 1H), 7.32 (t, $J = 7.5$ Hz, 1H), 6.00 (d, $J = 4.7$ Hz, 1H), 5.05 (dd, $J = 7.8$ and 3.7 Hz, 1H), 4.62−4.57 (m, 1H), 4.52−4.47 (m, 1H), 2.31 (t, $J = 7.3$ Hz, 2H), 1.94 (t, $J = 7.4$ Hz, 2H), 1.59 (t, $J = 6.7$ Hz, 2H), 1.50 (t, $J = 6.4$ Hz, 2H), 1.29 (br s, 4H). ^{13}C NMR (DMSO-d_6, 100 MHz) δ (ppm): 171.3, 169.1, 144.9, 130.5, 128.9, 125.5, 125.2, 121.6, 121.5, 119.3, 70.7, 56.4, 32.3, 28.4, 25.0. ESI-HRMS calculated for $[C_{24}H_{28}Br_1N_5O_4 + Na]^+$: 552.1217; found: 552.1210.

7-(3-Ethynylphenylcarbamoyl)heptanoic Acid Methyl Ester (8). Compound **8** (yield 37%) was prepared according to the methodology described for the preparation of compound **3**, by substituting 4-ethynylaniline (**1**) with 3-ethynylaniline (**7**). $R_f = 0.40$ (1:1 hexane:EtOAc). ^{1}H NMR (DMSO-d_6, 400 MHz) δ (ppm): 9.94 (s, 1H), 7.78 (s, 1H), 7.54 (d, $J = 8.0$ Hz, 1H), 7.29 (t, $J = 7.6$ Hz, 1H), 7.12 (d, $J = 7.6$ Hz, 1H), 4.14 (s, 1H), 3.56 (s, 3H), 2.28 (t, $J = 7.6$ Hz, 4H), 1.58−1.50 (m, 4H), 1.28 (br s, 4H). ^{13}C NMR (DMSO-d_6, 100 MHz) δ (ppm): 173.7, 171.9, 139.5, 129.5, 126.6, 125.8, 122.3, 122.2, 120.1, 83.8, 80.6, 51.5, 36.7, 33.6, 28.7, 28.6, 25.2, 24.7.

7-[3-(1-Benzyl-1*H*-[1,2,3]triazol-4-yl)phenylcarbamoyl]heptanoic Acid Methyl Ester (9a). Compound **9a** (yield 58%) was prepared according to the methodology described for the preparation of compound **5a** by substituting **3** with **8**. $R_f = 0.64$ (1:2 hexane: EtOAc). ^{1}H NMR (DMSO-d_6, 400 MHz) δ (ppm): 9.95 (s, 1H), 8.58 (s, 1H), 8.14 (s, 1H), 7.54 (d, $J = 8.0$ Hz, 1H), 7.45 (d, $J = 8.0$ Hz, 1H), 7.41−7.31 (m, 6H), 5.63 (s, 2H), 3.56 (s, 3H), 2.32−2.27 (m, 4H), 1.60−1.50 (m, 4H), 1.30 (br s, 4H). ^{13}C NMR (DMSO-d_6, 100 MHz) δ (ppm): 171.7, 147.0, 140.2, 136.4, 131.4, 129.6, 129.2, 128.6, 128.3, 125.9, 125.8, 121.9, 120.4, 118.9, 116.0, 53.4, 51.6, 36.7, 33.6, 28.7, 28.6, 25.3, 24.7.

7-{3-[1-(4-Fluorobenzyl)-1*H*-[1,2,3]triazol-4-yl]phenylcarbamoyl}-heptanoic Acid Methyl Ester (9b). Compound **9b** (yield 37%) was prepared according to the methodology described for the preparation of compound **5b,** by substituting **3** with **8**. $R_f = 0.61$ (1:2 hexane: EtOAc). ^{1}H NMR (DMSO-d_6, 400 MHz) δ (ppm): 9.94 (s, 1H), 8.57 (s, 1H), 8.13 (s, 1H), 7.53 (d, $J = 7.6$ Hz, 1H), 7.45−7.41 (m, 3H), 7.33 (t, $J = 8.0$ Hz, 1H), 7.24−7.19 (m, 2H), 5.62 (s, 2H), 3.56 (s, 3H), 2.31−2.27 (m, 4H), 1.59−1.48 (m, 4H), 1.25 (br s, 4H). ^{13}C NMR (DMSO-d_6, 100 MHz) δ (ppm): 173.7, 171.7, 147.0, 140.2, 131.4, 130.7, 129.6, 121.9, 120.4, 118.9, 116.1, 115.9, 52.6, 51.6, 36.7, 33.6, 28.7, 28.6, 25.3, 24.7.

7-[3-(1-Phenyl-1*H*-[1,2,3]triazol-4-yl)phenylcarbamoyl]heptanoic Acid Methyl Ester (9c). Compound **9c** (yield 56%) was prepared according to the methodology described for the preparation of compound **5c** by substituting **3** with **8**. $R_f = 0.78$ (1:2 hexane: EtOAc). ^{1}H NMR (DMSO-d_6, 400 MHz) δ (ppm): 10.00 (s, 1H), 9.25 (s, 1H), 8.25 (s, 1H), 7.97 (d, $J = 7.6$ Hz, 2H), 7.65−7.49 (m, 5H), 7.40 (t, $J = 7.6$ Hz, 1H), 3.57 (s, 3H), 2.34−2.28 (m, 4H), 1.60 (t, $J = 6.8$ Hz, 2H), 1.53 (t, $J = 7.2$ Hz, 2H), 1.31 (br s, 4H). ^{13}C NMR (DMSO-d_6, 100 MHz) δ (ppm): 171.8, 147.7, 140.3, 137.0, 131.0, 130.3, 129.7, 129.1, 125.8, 120.7, 120.4, 120.0, 119.3, 116.3, 51.6, 36.7, 33.6, 28.7, 28.6, 25.3, 24.7.

7-(3-{1-[2-(3-Bromophenyl)-2-hydroxyethyl]-1*H*-[1,2,3]triazol-4-yl}phenylcarbamoyl)heptanoic Acid Methyl Ester (9d). Compound **9d** (yield 71%) was prepared according to the methodology described for the preparation of compound **5d** by substituting **3** with **8**. $R_f = 0.52$ (1:2 hexane:EtOAc). ^{1}H NMR (CD_3OD, 400 MHz) δ (ppm): 8.24 (s, 1H), 7.99 (s, 1H), 7.60 (s, 1H), 7.57 (dd, $J = 8.0$ and 0.8 Hz, 1H), 7.53 (d, $J = 8.0$ Hz, 1H), 7.46 (d, $J = 8.0$ Hz, 1H), 7.38 (t, $J = 8.0$ Hz, 2H), 7.27 (t, $J = 8.0$ Hz, 1H), 5.11 (dd, $J = 8.0$ and 4.0 Hz, 1H), 4.67−4.64 (m, 1H), 4.61−4.57 (m, 1H), 3.65 (s, 3H), 2.40 (t, $J = 7.6$ Hz, 2H), 2.34 (t, $J = 7.2$ Hz, 2H), 1.72 (t, $J = 7.2$ Hz, 2H), 1.64 (t, $J = 7.2$ Hz, 2H), 1.41 (br s, 4H). ^{13}C NMR (CD_3OD, 100 MHz) δ (ppm): 173.2, 143.8, 139.1, 130.9, 130.6, 129.9, 129.0, 128.7, 124.5, 122.1, 122.0, 120.9, 119.5, 116.8, 71.4, 56.8, 50.5, 36.4, 33.2, 28.5, 28.4, 25.2, 24.4.

Octanedioic Acid [3-(1-Benzyl-1*H*-[1,2,3]triazol-4-yl)phenyl]-amide Hydroxyamide (10a). Compound **10a** (yield 36%) was prepared according to the methodology described for the preparation of compound **6a**. ^{1}H NMR (DMSO-d_6, 400 MHz) δ (ppm): 10.33 (s, 1H), 9.96 (s, 1H), 8.59 (s, 1H), 8.15 (s, 1H), 7.55 (d, $J = 8.0$ Hz, 1H), 7.46 (d, $J = 8.0$ Hz, 1H), 7.41−7.32 (m, 5H), 5.64 (s, 2H), 2.31 (t, $J = 8.0$ Hz, 2H), 1.94 (t, $J = 8.0$ Hz, 2H), 1.58 (t, $J = 8.0$ Hz, 2H), 1.49 (t, $J = 8.0$ Hz, 2H), 1.28 (br s, 4H). ^{13}C NMR

(DMSO-d_6, 100 MHz) δ (ppm): 171.8, 169.5, 147.0, 140.2, 136.4, 131.4, 129.6, 129.2, 128.6, 128.3, 125.8, 121.9, 120.4, 118.9, 116.1, 53.4, 36.8, 32.6, 28.8, 25.4. ESI-HRMS calculated for $[C_{23}H_{27}N_5O_3 + H]^+$: 422.2186; found: 422.2180.

Octanedioic Acid {3-[1-(4-Fluorobenzyl)-1*H*-[1,2,3]triazol-4-yl]phenyl}amide Hydroxyamide (10b). Compound **10d** (yield 34%) was prepared according to the methodology described for the preparation of compound **6a**. ^{1}H NMR (CD_3OD, 400 MHz) δ (ppm): 8.31 (s, 1H), 8.02 (s, 1H), 7.54 (d, J = 7.6 Hz, 2H), 7.44 (dd, J = 8.4 and 5.2 Hz, 2H), 7.38 (t, J = 8.0 Hz, 1H), 7.14 (t, J = 8.8 Hz, 2H), 5.64 (s, 2H), 2.40 (t, J = 7.2 Hz, 2H), 2.11 (t, J = 7.6 Hz, 2H), 1.74−1.63 (m, 4H), 1.42 (br s, 4H). ^{13}C NMR (CD_3OD, 100 MHz) δ (ppm): 172.9, 171.1, 163.5, 161.2, 147.2, 138.7, 131.0, 130.4, 129.5, 128.6, 120.5, 119.2, 116.5, 115.1, 114.8, 99.5, 52.4, 36.0, 31.8, 28.0, 24.8, 24.7. ESI-HRMS calculated for $[C_{23}H_{26}F_1N_5O_3 + H]^+$: 440.2092; found: 440.2088.

Octanedioic Acid Hydroxyamide [3-(1-Phenyl-1*H*-[1,2,3]triazol-4-yl)phenyl]amide (10c). Compound **10c** (yield 47%) was prepared according to the methodology described for the preparation of compound **6a**. ^{1}H NMR (DMSO-d_6, 400 MHz) δ (ppm): 10.34 (s, 1H), 10.03 (s, 1H), 9.27 (s, 1H), 8.66 (s, 1H), 8.27 (s, 1H), 7.98 (d, J = 7.6 Hz, 2H), 7.66−7.50 (m, 5H), 7.41 (t, J = 7.6 Hz, 1H), 2.33 (t, J = 7.2 Hz, 2H), 1.95 (t, J = 7.2 Hz, 2H), 1.61 (t, J = 6.4 Hz, 2H), 1.50 (t, J = 6.8 Hz, 2H), 1.30 (br s, 4H). ^{13}C NMR (DMSO-d_6, 100 MHz) δ (ppm): 171.4, 169.1, 147.3, 140.0, 136.7, 130.7, 129.9, 129.4, 128.7, 120.3, 120.0, 119.6, 119.0, 115.9, 99.5, 36.4, 32.3, 28.4, 25.0. ESI-HRMS calculated for $[C_{22}H_{25}N_5O_3 + H]^+$: 408.2030; found: 408.2033.

Octanedioic Acid (3-{1-[2-(3-Bromophenyl)-2-hydroxyethyl]-1*H*-[1,2,3]triazol-4-yl}phenyl)amide Hydroxyamide (10d). Compound **10d** (yield 56%) was prepared according to the methodology described for the preparation of compound **6a**. ^{1}H NMR (DMSO-d_6, 400 MHz) δ (ppm): 10.34 (s, 1H), 9.98 (s, 1H), 8.45 (s, 1H), 8.16 (s, 1H), 7.62 (s, 1H), 7.55 (d, J = 7.6 Hz, 1H), 7.50−7.45 (m, 3H), 7.39 (t, J = 6.8 Hz, 1H), 7.37−7.31 (m, 2H), 5.07 (br s, 1H), 4.59−4.52 (m, 2H), 2.32 (t, J = 6.4 Hz, 2H), 1.95 (t, J = 7.2 Hz, 2H), 1.60 (br s, 2H), 1.50 (br s, 2H), 1.29 (br s, 4H). ^{13}C NMR (DMSO-d_6, 100 MHz) δ (ppm): 171.4, 169.1, 146.0, 144.9, 139.9, 131.2, 130.5, 129.3, 128.9, 125.2, 122.1, 121.6, 119.9, 118.4, 115.6, 70.7, 56.4, 36.4, 32.3, 28.4, 25.1. ESI-HRMS calculated for $[C_{24}H_{28}Br_1N_5O_4 + H]^+$: 530.1397; found: 530.1388.

7-[4-(3-Benzyl-3*H*-[1,2,3]triazol-4-yl)phenylcarbamoyl]heptanoic Acid Methyl Ester (11a). A mixture of benzyl azide (**4a**, 139 mg, 1.04 mmol), phenylacetylene **3** (100 mg, 0.35 mmol), and Cp*RuCl-(PPh_3)$_2$ (83 mg, 0.10 mmol) was refluxed in 20 mL of THF for 8 h under argon. The progress of reaction was monitored by TLC, and phenylacetylene **3** was consumed completely at the end of reaction. The solvent was removed under vacuum, and the crude solid was purified by preparative TLC to give compound **11a** (89 mg, 61%). R_f = 0.45 (1:2 hexane:EtOAc). ^{1}H NMR ($CDCl_3$, 400 MHz) δ (ppm): 8.62 (s, 1H), 7.71 (s, 1H), 7.69 (d, J = 8.4 Hz, 2H), 7.27−7.26 (m, 3H), 7.19 (d, J = 8.4 Hz, 2H), 7.08−7.06 (m, 2H), 5.53 (s, 2H), 3.64 (s, 3H), 2.40 (t, J = 7.2 Hz, 2H), 2.29 (d, J = 7.6 Hz, 2H), 1.72 (t, J = 6.8 Hz, 2H), 1.61 (t, J = 7.2 Hz, 2H), 1.36 (br s, 4H). ^{13}C NMR ($CDCl_3$, 100 MHz) δ (ppm): 173.8, 171.7, 139.4, 137.7, 135.0, 132.5, 129.0, 128.4, 128.2, 127.8, 126.6, 121.2, 119.5, 51.3, 51.1, 36.9, 33.5, 28.3, 24.8, 24.2.

7-{4-[3-(4-Fluorobenzyl)-3*H*-[1,2,3]triazol-4-yl]phenylcarbamoyl}-heptanoic Acid Methyl Ester (11b). Compound **11b** (yield 50%) was prepared according to the methodology described for the preparation of compound **11a** by substituting **4a** with 4-fluorobenzyl azide (**4b**). R_f = 0.45 (1:2 hexane:EtOAc). ^{1}H NMR ($CDCl_3$, 400 MHz) δ (ppm): 8.38 (s, 1H), 7.70 (s, 1H), 7.68 (d, J = 8.4 Hz, 2H), 7.19 (d, J = 8.4 Hz, 2H), 7.08−7.04 (m, 2H), 6.97−6.93 (m, 2H), 5.50 (s, 2H), 3.65 (s, 3H), 2.40 (t, J = 7.6 Hz, 2H), 2.30 (t, J = 7.6 Hz, 2H), 1.73 (t, J = 6.8 Hz, 2H), 1.62 (t, J = 7.2 Hz, 2H), 1.37 (br s, 4H). ^{13}C NMR ($CDCl_3$, 100 MHz) δ (ppm): 173.8, 171.6, 163.3, 160.8, 139.4, 137.5, 132.7, 130.7, 129.0, 128.7, 128.6, 121.2, 119.4, 115.5, 115.3, 51.1, 50.7, 37.0, 33.5, 28.3, 28.2, 24.8, 24.2.

7-[4-(3-Phenyl-3*H*-[1,2,3]triazol-4-yl)phenylcarbamoyl]heptanoic Acid Methyl Ester (11c). A mixture of phenylazide (**4c**, 1.65 g, 13.9 mmol) and phenylacetylene **3** (200 mg, 0.69 mmol) in 20 mL of toluene was heated to refluxed for 2 days. The toluene was removed under vacuum, and the crude mixture was purified by preparative TLC to give compound **11c** (65 mg, yield 23%, R_f = 0.53, hexane:EtOAc 1:2) and compound **5c** (57 mg, yield 20%, R_f = 0.70, hexane:EtOAc 1:2). Compound **11c**: ^{1}H NMR (CD_3OD, 400 MHz) δ (ppm): 7.96 (s, 1H), 7.58 (d, J = 8.8 Hz, 2H), 7.53−7.50 (m, 3H), 7.40−7.38 (m, 2H), 7.21 (d, J = 8.8 Hz, 2H), 3.63 (s, 3H), 2.36 (t, J = 7.2 Hz, 2H), 2.31 (t, J = 7.6 Hz, 2H), 1.66 (t, J = 7.2 Hz, 2H), 1.61 (t, J = 7.2 Hz, 2H), 1.37 (br s, 4H). ^{13}C NMR (CD_3OD, 100 MHz) δ (ppm): 174.0, 172.9, 139.4, 137.7, 136.1, 131.9, 129.0, 128.8, 128.5, 124.9, 120.9, 119.1, 50.1, 36.1, 32.8, 28.1, 28.0, 24.7, 24.0.

7-(4-{3-[2-(3-Bromo-phenyl)-2-hydroxyethyl]-3*H*-[1,2,3]triazol-4-yl}phenylcarbamoyl)heptanoic Acid Methyl Ester (11d). Compound **11d** (yield 40%) was prepared according to the methodology described for the preparation of compound **11a** by substituting **4a** with 2-azido-1-(3-bromophenyl)ethanol (**4d**). R_f = 0.30 (1:2 hexane: EtOAc). ^{1}H NMR ($CDCl_3$, 400 MHz) δ (ppm): 8.60 (s, 1H), 7.67 (d, J = 8.4 Hz, 2H), 7.52 (s, 1H), 7.40 (s, 1H), 7.34 (d, J = 6.8 Hz, 1H), 7.23 (d, J = 8.0 Hz, 2H), 7.12−7.10 (m, 3H), 5.29 (br s, 1H), 4.98 (br s, 1H), 4.45−4.40 (m, 2H), 3.63 (s, 3H), 2.37 (t, J = 7.2 Hz, 2H), 2.28 (t, J = 7.2 Hz, 2H), 1.69 (t, J = 6.4 Hz, 2H), 1.59 (t, J = 6.8 Hz, 2H), 1.34 (br s, 4H). ^{13}C NMR ($CDCl_3$, 100 MHz) δ (ppm): 174.0, 171.8, 142.5, 139.3, 138.5, 131.9, 130.7, 129.7, 129.3, 128.5, 124.2, 122.3, 121.0, 119.6, 71.6, 54.3, 51.1, 36.0, 33.5, 28.3, 24.8, 24.2.

Octanedioic Acid [4-(3-Benzyl-3*H*-[1,2,3]triazol-4-yl)phenyl]-amide Hydroxyamide (12a). Compound **12a** (yield 57%) was prepared according to the methodology described for the preparation of compound **6a**. ^{1}H NMR (CD_3OD, 400 MHz) δ (ppm): 7.82 (s, 1H), 7.67 (d, J = 8.4 Hz, 2H), 7.30 (d, J = 8.4 Hz, 2H), 7.27−7.25 (m, 3H), 7.04−7.02 (m, 2H), 5.64 (s, 2H), 2.39 (t, J = 7.2 Hz, 2H), 2.10 (t, J = 7.2 Hz, 2H), 1.70 (t, J = 7.2 Hz, 2H), 1.63 (t, J = 6.8 Hz, 2H), 1.39 (br s, 4H). ^{13}C NMR(CD_3OD, 75 MHz) δ (ppm): 173.0, 171.1, 139.6, 137.9, 135.1, 131.9, 128.7, 128.0, 127.4, 126.3, 120.9, 119.3, 51.2, 36.1, 31.8, 28.1, 28.0, 24.7. ESI-HRMS calculated for $[C_{23}H_{27}N_5O_3 + Na]^+$: 444.2006; found: 444.2007.

Octanedioic Acid {4-[3-(4-Fluorobenzyl)-3*H*-[1,2,3]triazol-4-yl]phenyl}amide Hydroxyamide (12b). Compound **12b** (yield 66%) was prepared according to the methodology described for the preparation of compound **6a**. ^{1}H NMR (CD_3OD, 400 MHz) δ (ppm): 9.97 (s, 1H), 7.80 (s, 1H), 7.70−7.67 (m, 2H), 7.32 (d, J = 8.4 Hz, 2H), 7.09−7.05 (m, 2H), 7.03−6.98 (m, 2H), 5.64 (s, 2H), 2.40 (t, J = 7.6 Hz, 2H), 2.10 (t, J = 7.2 Hz, 2H), 1.71 (t, J = 6.8 Hz, 2H), 1.64 (t, J = 7.2 Hz, 2H), 1.41 (br s, 4H). ^{13}C NMR (CD_3OD, 100 MHz) δ (ppm): 173.3, 171.5, 163.8, 161.2, 140.0, 138.1, 132.5, 131.5, 129.1, 129.0, 128.9, 125.8, 121.4, 119.7, 115.2, 115.0, 50.8, 36.4, 32.2, 28.4, 28.3, 25.1. ESI-HRMS calculated for $[C_{23}H_{26}F_1N_5O_3 + H]^+$: 440.2092; found: 440.2087.

Octanedioic Acid Hydroxyamide [3-(3-Phenyl-3*H*-[1,2,3]triazol-4-yl)phenyl]amide (12c). Compound **12c** (yield 57%) was prepared according to the methodology described for the preparation of compound **6a**. ^{1}H NMR (CD_3OD, 400 MHz) δ (ppm): 7.97 (s, 1H), 7.58 (d, J = 8.4 Hz, 2H), 7.54−7.51 (m, 3H), 7.41−7.38 (m, 2H), 7.22 (d, J = 8.4 Hz, 2H), 2.37 (t, J = 7.2 Hz, 2H), 2.09 (t, J = 7.6 Hz, 2H), 1.69−1.61 (m, 4H), 1.39 (br s, 4H). ^{13}C NMR (CD_3OD, 100 MHz) δ (ppm): 173.3, 171.5, 139.8, 138.1, 136.4, 132.2, 129.4, 129.2, 128.9, 125.8, 125.3, 121.3, 119.5, 36.4, 32.2, 28.4, 28.4, 25.1. ESI-HRMS calculated for $[C_{22}H_{25}N_5O_3 + H]^+$: 408.2030; found: 408.2026.

Octanedioic Acid (4-{3-[2-(3-Bromophenyl)-2-hydroxy-ethyl]-3*H*-[1,2,3]triazol-4-yl}phenyl)amide Hydroxyamide (12d). Compound **12d** (yield 41%) was prepared according to the methodology described for the preparation of compound **6a**. ^{1}H NMR (DMSO-d_6, 400 MHz) δ (ppm): 10.32 (s, 1H), 10.06 (s, 1H), 8.64 (br s, 1H), 7.75 (s, 1H), 7.71 (d, J = 8.8 Hz, 2H), 7.43 (d, J = 7.6 Hz, 1H), 7.38 (d, J = 8.8 Hz, 2H), 7.34 (s, 1H), 7.23 (t, J = 7.6 Hz, 1H), 7.13 (d, J = 8.0 Hz, 1H), 5.93 (d, J = 4.0 Hz, 1H), 4.97 (br

s, 1H), 4.49−4.46 (m, 2H), 2.32 (t, J = 7.2 Hz, 2H), 1.93 (t, J = 7.2 Hz, 2H), 1.58 (t, J = 6.4 Hz, 2H), 1.49 (t, J = 6.8 Hz, 2H), 1.28 (br s, 4H). ^{13}C NMR (100 MHz, DMSO-d_6): 172.0, 169.5, 145.1, 140.6, 138.4, 132.6, 130.8, 129.6, 129.0, 125.4, 122.0, 121.4, 119.4, 71.2, 54.7, 36.8, 32.6, 28.8, 25.4. ESI-HRMS calculated for $[C_{24}H_{28}Br_1N_5O_4 + H]^+$: 530.1397; found: 530.1391.

7-[3-(3-Benzyl-3*H*-[1,2,3]triazol-4-yl)phenylcarbamoyl]heptanoic Acid Methyl Ester (13a). Compound **13a** (yield 38%) was prepared according to the methodology described for the preparation of compound **11a** by substituting **3** with **8**. R_f = 0.55 (1:2 hexane:EtOAc). ^{1}H NMR ($CDCl_3$, 300 MHz) δ (ppm): 8.56 (s, 1H), 7.72−7.68 (m, 2H), 7.63 (d, J = 8.2 Hz, 1H), 7.30 (t, J = 7.8 Hz, 1H), 7.24−7.21 (m, 3H), 7.06−7.03 (m, 2H), 6.92 (d, J = 7.5 Hz, 1H), 5.56 (s, 2H), 3.64 (s, 3H), 2.38 (t, J = 7.3 Hz, 2H), 2.31 (t, J = 6.6 Hz, 2H), 1.68 (t, J = 6.9 Hz, 2H), 1.60 (t, J = 6.7 Hz, 2H), 1.35 (br s, 4H). ^{13}C NMR ($CDCl_3$, 75 MHz) δ (ppm): 174.7, 172.5, 139.5, 138.5, 135.6, 133.5, 129.9, 129.1, 128.5, 127.7, 127.5, 124.3, 121.1, 120.5, 52.3, 37.7, 34.3, 29.1, 25.6, 25.0.

7-{3-[3-(4-Fluorobenzyl)-3*H*-[1,2,3]triazol-4-yl]phenylcarbamoyl}heptanoic Acid Methyl Ester (13b). Compound **13b** (yield 55%) was prepared according to the methodology described for the preparation of compound **11a**, by substituting **3** with **8**. R_f = 0.55 (1:2 hexane:EtOAc). ^{1}H NMR ($CDCl_3$, 300 MHz) δ (ppm): 8.71 (s, 1H), 7.75 (s, 1H), 7.68 (s, 1H), 7.56 (d, J = 8.0 Hz, 1H), 7.30 (t, J = 7.9 Hz, 1H), 7.05−7.00 (m, 2H), 6.92−6.86 (m, 3H), 5.52 (s, 2H), 3.62 (s, 3H), 2.38 (t, J = 7.3 Hz, 2H), 2.27 (t, J = 7.3 Hz, 2H), 1.68 (t, J = 6.8 Hz, 2H), 1.59 (t, J = 6.7 Hz, 2H), 1.33 (br s, 4H). ^{13}C NMR ($CDCl_3$, 75 MHz) δ (ppm): 174.7, 172.6, 161.1, 139.6, 138.4, 133.5, 131.3, 129.9, 129.8, 129.7, 127.4, 124.3, 121.1, 120.5, 116.2, 115.9, 51.9, 51.6, 37.6, 34.3, 29.1, 25.6, 25.0.

7-[3-(3-Phenyl-3*H*-[1,2,3]triazol-4-yl)phenylcarbamoyl]heptanoic Acid Methyl Ester (13c). Compound **13c** (yield 16%, R_f = 0.59, hexane:EtOAc 1:2) was prepared according to the methodology described for the preparation of compound **11c**, together with its regioisomer **9c** (yield 12%, R_f = 0.78, hexane:EtOAc 1:2). Compound **13c**: ^{1}H NMR ($CDCl_3$, 400 MHz) δ (ppm): 7.84 (s, 1H), 7.61 (d, J = 8.0 Hz, 1H), 7.58 (s, 1H), 7.44−7.41 (m, 3H), 7.38−7.36 (m, 2H), 7.25 (t, J = 8.0 Hz, 1H), 6.83 (d, J = 7.6 Hz, 1H), 3.66 (s, 3H), 2.35 (t, J = 7.2 Hz, 2H), 2.31 (t, J = 7.6 Hz, 2H), 1.71 (t, J = 6.8 Hz, 2H), 1.62 (t, J = 6.8 Hz, 2H), 1.35 (br s, 4H). ^{13}C NMR (CD_3OD, 100 MHz) δ (ppm): 173.8, 171.2, 138.5, 137.1, 136.0, 133.1, 129.0, 128.9, 126.9, 124.7, 123.6, 120.0, 119.2, 51.1, 37.0, 33.5, 28.2, 24.8, 24.2.

7-(3-{3-[2-(3-Bromophenyl)-2-hydroxyethyl]-3*H*-[1,2,3]triazol-4-yl}phenylcarbamoyl)heptanoic Acid Methyl Ester (13d). Compound **13d** (yield 43%) was prepared according to the methodology described for the preparation of compound **11a**, by substituting **3** with **8**. R_f = 0.35 (1:2 hexane:EtOAc). ^{1}H NMR (CD_3OD, 400 MHz) δ (ppm): 7.71 (s, 1H), 7.62 (s, 1H), 7.58 (d, J = 8.0 Hz, 1H), 7.42 (t, J = 8.0 Hz, 1H), 7.36 (d, J = 8.0 Hz, 1H), 7.13 (t, J = 7.6 Hz, 1H), 7.06 (t, J = 7.2 Hz, 2H), 5.05 (t, J = 6.4 Hz, 1H), 4.70−4.65 (m, 1H), 4.60−4.55 (m, 1H), 3.64 (s, 3H), 2.41 (t, J = 7.2 Hz, 2H), 2.33 (t, J = 7.6 Hz, 2H), 1.74 (t, J = 6.8 Hz, 2H), 1.64 (t, J = 7.2 Hz, 2H), 1.42 (br s, 4H). ^{13}C NMR ($CDCl_3$, 100 MHz) δ (ppm): 173.9, 171.7, 142.3, 138.5, 138.4, 132.1, 131.6, 131.5, 131.0, 129.7, 129.2, 128.6, 128.3, 128.1, 126.5, 124.2, 123.9, 122.2, 120.3, 119.8, 71.7, 54.5, 51.1, 36.9, 33.5, 28.4, 28.3, 24.8, 24.2.

Octanedioic Acid [3-(3-Benzyl-3*H*-[1,2,3]triazol-4-yl)phenyl]amide Hydroxyamide (14a). Compound **14a** (yield 66%) was prepared according to the methodology described for the preparation of compound **6a**. ^{1}H NMR (CD_3OD, 400 MHz) δ (ppm): 10.32 (s, 1H), 10.01 (s, 1H), 8.65 (br s, 1H), 7.90 (s, 1H), 7.77 (s, 1H), 7.61 (d, J = 8.0 Hz, 1H), 7.38 (t, J = 8.0 Hz, 1H), 7.29−7.22 (m, 5H), 7.09 (d, J = 7.6 Hz, 1H), 7.01 (d, J = 6.4 Hz, 2H), 5.66 (s, 2H), 2.29 (t, J = 7.2 Hz, 2H), 1.93 (t, J = 7.2 Hz, 2H), 1.57 (t, J = 6.4 Hz, 2H), 1.48 (t, J = 6.4 Hz, 2H), 1.27 (br s, 4H). ^{13}C NMR (CD_3OD, 100 MHz) δ (ppm): 171.9, 171.8, 140.2, 140.1, 138.0, 136.3, 133.3, 129.9, 129.0, 128.2, 127.4, 127.2, 125.8, 123.3, 120.2, 119.4, 119.3, 51.6, 36.8, 32.6, 28.8, 25.4, 25.3. ESI-HRMS calculated for $[C_{23}H_{27}N_5O_3 + H]^+$: 422.2186; found: 422.2181.

Octanedioic Acid {4-[3-(4-Fluorobenzyl)-3*H*-[1,2,3]triazol-4-yl]phenyl}amide Hydroxyamide (14b). Compound **14b** (yield 44%) was prepared according to the methodology described for the preparation of compound **6a**. ^{1}H NMR (CD_3OD, 400 MHz) δ (ppm): 10.32 (s, 1H), 10.02 (s, 1H), 7.90 (s, 1H), 7.75 (s, 1H), 7.61 (d, J = 8.0 Hz, 1H), 7.39 (t, J = 8.0 Hz, 1H), 7.12−7.04 (m, 5H), 5.65 (s, 2H), 2.29 (t, J = 7.2 Hz, 2H), 1.93 (t, J = 7.2 Hz, 2H), 1.57 (t, J = 6.8 Hz, 2H), 1.48 (t, J = 7.2 Hz, 2H), 1.27 (br s, 4H). ^{13}C NMR (CD_3OD, 100 MHz) δ (ppm): ESI-HRMS calculated for $[C_{23}H_{26}F_1N_5O_3 + H]^+$: 462.1911; found: 462.1912.

Octanedioic Acid Hydroxyamide [4-(3-Phenyl-3*H*-[1,2,3]triazol-4-yl)phenyl]amide (14c). Compound **14c** (yield 42%) was prepared according to the methodology described for the preparation of compound **6a**. ^{1}H NMR (DMSO-d_6, 400 MHz) δ (ppm): 10.31 (s, 1H), 9.96 (s, 1H), 8.64 (s, 1H), 8.05 (s, 1H), 7.64 (s, 1H), 7.59 (d, J = 8.4 Hz, 1H), 7.53−7.51 (m, 3H), 7.40−7.39 (m, 2H), 7.27 (t, J = 7.6 Hz, 1H), 6.84 (d, J = 7.6 Hz, 1H), 2.25 (t, J = 7.2 Hz, 2H), 1.92 (t, J = 7.2 Hz, 2H), 1.53−1.47 (m, 4H), 1.24 (br s, 4H). ^{13}C NMR (DMSO-d_6, 100 MHz) δ (ppm): 171.8, 169.5, 140.2, 138.0, 136.6, 133.5, 130.0, 129.9, 129.6, 127.2, 125.8, 123.4, 120.0, 119.3, 36.7, 32.6, 28.8, 28.7, 25.4, 25.3. ESI-HRMS calculated for $[C_{22}H_{25}N_5O_3 + Na]^+$: 430.1849; found: 430.1845.

Octanedioic Acid (4-{3-[2-(3-Bromophenyl)-2-hydroxyethyl]-3*H*-[1,2,3]triazol-4-yl}phenyl)amide Hydroxyamide (14d). Compound **12b** (yield 49%) was prepared according to the methodology described for the preparation of compound **6a**. ^{1}H NMR (CD_3OD, 400 MHz) δ (ppm): 7.71 (s, 1H), 7.67 (s, 1H), 7.58 (d, J = 8.4 Hz, 1H), 7.41 (t, J = 8.0 Hz, 1H), 7.36 (d, J = 8.0 Hz, 1H), 7.30 (s, 1H), 7.12 (t, J = 7.6 Hz, 1H), 7.06 (t, J = 7.2 Hz, 2H), 5.05 (t, J = 6.8 Hz, 1H), 4.69−4.64 (m, 1H), 4.59−4.54 (m, 1H), 2.41 (t, J = 7.6 Hz, 2H), 2.10 (t, J = 7.2 Hz, 2H), 1.73 (t, J = 6.8 Hz, 2H), 1.66 (t, J = 7.6 Hz, 2H), 1.42 (br s, 4H). ^{13}C NMR (CD_3OD, 100 MHz) δ (ppm): 173.3, 171.5, 143.6, 139.1, 139.0, 131.9, 130.6, 129.7, 129.1, 128.7, 126.8, 124.5, 124.0, 122.0, 120.5, 120.1, 71.5, 54.4, 36.4, 32.2, 28.5, 28.4, 25.2, 25.1. ESI-HRMS calculated for $[C_{24}H_{28}Br_1N_5O_4 + H]^+$: 530.1397; found: 530.1392.

Biological Methods. HDAC Inhibition Assay. The inhibitory effects of compounds on histone deacetylase (HDAC) activity were determined using a fluorescence-based assay with electrophoretic separation of substrate and product carried out using a microfluidic system followed by quantitation of fluorescence intensity in the substrate and product peaks. The assays were performed using isolated HDAC isoforms that had been expressed as 6× His-tagged fusion proteins in a baculovirus expression system in Sf9 cells. HDACs 1, 2, 3, 6, and 8 were expressed as full length fusion proteins. The HDAC10 fusion protein was expressed as a carboxy-terminal deletion of 38 amino acids (residues 632−669). HDAC3 was coexpressed with a fragment of the SMRT gene (residues 395−489) to generate enzymatically active protein. Purified proteins were incubated with 1 μM carboxyfluorescein (FAM)-labeled acetylated peptide substrate and test compound for 17 h at 25 °C in HDAC assay buffer containing 100 mM HEPES (pH 7.5), 25 mM KCl, 0.1% BSA, and 0.01% Triton X-100. Reactions were terminated by the addition of buffer containing 0.078% SDS for a final SDS concentration of 0.05%. Substrate and product were separated electrophoretically using a Caliper LabChip 3000 system with blue laser excitation and green fluorescence detection (CCD2). The fluorescence intensity in the substrate and product peaks was determined using the Well Analyzer software on the Caliper system. The reactions were performed in duplicate for each sample. IC_{50} values were automatically calculated using the IDBS XLFit version 4.2.1 plug-in for Microsoft Excel and the XLFit 4 Parameter Logistic Model (Sigmoidal Dose−Response Model): $((A + ((B - A)/1 + ((C/x)^D))))$, where x is compound concentration, A is the estimated minimum and B is the estimated maximum of % inhibition, C is the inflection point, and D is the Hill slope of the sigmoidal curve. The standard errors of the IC_{50}s were automatically calculated using the IDBS XLFit version 4.2.1 plug-in for Microsoft Excel and the formula xf4_FitResultStdError().

Cytotoxicity Assays. The pancreatic cancer cell lines BxPc-3, HupT3, MiaPaCa-2, Panc 04.03, and SU86.86 were obtained from

ATCC (Rockville, MD) and were grown in medium (DMEM or RPMI) containing 10% fetal calf serum and L-glutamine. Pancreatic cancer cells were plated out in duplicate into 6 wells of a 96-well microtiter plate at 2.5−4 × 103 cells per well. Four-hours post plating, individual wells were treated with diluent (DMSO) or varying concentrations of SAHA or the indicated HDACIs from a concentration of 1 nm to 50 μM. Cytotoxicity was measured at time "0" and 72 h post treatment using the colorimetric MTS assay according to the manufacturer's suggestions (Promega, Madison, WI). The IC_{50}s were calculated using XLfit (IDBS Limited, Guildford, UK).

Parasite Growth Inhibition Assay. The in vitro activities of HDAC inhibitors against *P. falciparum* strains W2, D6, TM91C235 and TM90C2A were evaluated using the method the labeled hypoxanthine assay of Desjardins et al.,[49] as modified by Milhous et al.[50] and described in one of our earlier papers.[51] W2 is chloroquine resistant and mefloquine sensitive, D6 is chloroquine sensitive but naturally less susceptible to mefloquine, TM91C235 is resistant to mefloquine, chloroquine, and pyrimethamine as is TM90C2A, however, this latter parasite is a two *pfmdr1* copy strain. Data are reported as a single IC_{50} value for each compound in Table 2. We routinely run mefloquine and chloroquine as controls to ensure assay validity. The IC_{50}s and standard deviations of chloroquine and mefloquine (for last 15 assays) for each strain are reported in Table 4. The selectivity index of each compound was calculated where possible using the following formula: SI = IC_{50} (mammalian cell line)/IC_{50} (*P. falciparum*).

Acknowledgment. We are indebted to the ADDF/Elan (grant no. 271210) for their support of these studies. We thank Dr. Rong He for assisting in the preparation of the manuscript, and Dr. Arsen Gaysin for providing technical support. This manuscript was reviewed by the WRAIR and the US Army Medical and Material Research Command and there is no objection to its publication or dissemination. The opinions expressed herein are those of the authors and do not reflect the views of the Department of the Army or the Department of Defense.

Supporting Information Available: The HPLC reports for the purity check of the final compounds measured in two different mobile phases. This material is available free of charge via the Internet at http://pubs.acs.org.

References

(1) Lehrmann, H.; Pritchard, L. L.; Harel-Bellan, A. Histone acetyltransferases and deacetylases in the control of cell proliferation and differentiation. *Adv. Cancer Res.* **2002**, *86*, 41–65.
(2) Gui, C. Y.; Ngo, L.; Xu, W. S.; Richon, V. M.; Marks, P. A. Histone deacetylase (HDAC) inhibitor activation of p21WAF1 involves changes in promoter-associated proteins, including HDAC1. *Proc. Natl. Acad. Sci. U.S.A.* **2004**, *101*, 1241–1246.
(3) Marks, P. A.; Dokmanovic, M. Histone deacetylase inhibitors: discovery and development as anticancer agents. *Expert Opin. Invest. Drugs* **2005**, *14*, 1497–1511.
(4) Minucci, S.; Pelicci, P. G. Histone deacetylase inhibitors and the promise of epigenetic (and more) treatments for cancer. *Nat. Rev. Cancer* **2006**, *6*, 38–51.
(5) Rundlett, S. E.; Carmen, A. A.; Kobayashi, R.; Bavykin, S.; Turner, B. M.; Grunstein, M. HDA1 and RPD3 are members of distinct yeast histone deacetylase complexes that regulate silencing and transcription. *Proc. Natl. Acad. Sci. U.S.A.* **1996**, *93*, 14503–14508.
(6) Taunton, J.; Hassig, C. A.; Schreiber, S. L. A mammalian histone deacetylase related to the yeast transcriptional regulator Rpd3p. *Science* **1996**, *272*, 408–411.
(7) Marks, P.; Rifkind, R. A.; Richon, V. M.; Breslow, R.; Miller, T.; Kelly, W. K. Histone deacetylases and cancer: causes and therapies. *Nat. Rev. Cancer* **2001**, *1*, 194–202.
(8) Yang, X. J.; Grâegoire, S. Class II histone deacetylases: from sequence to function, regulation, and clinical implication. *Mol. Cell. Biol.* **2005**, *25*, 2873–2884.
(9) Finnin, M. S.; Donigian, J. R.; Cohen, A.; Richon, V. M.; Rifkind, R. A.; Marks, P. A.; Breslow, R.; Pavletich, N. P. Structures of a histone deacetylase homologue bound to the TSA and SAHA inhibitors. *Nature* **1999**, *401*, 188–193.
(10) Frye, R. A. Phylogenetic classification of prokaryotic and eukaryotic Sir2-like proteins. *Biochem. Biophy. Res. Commun.* **2000**, *273*, 793–798.
(11) Gao, L.; Cueto, M. A.; Asselbergs, F.; Atadja, P. Cloning and functional characterization of HDAC11, a novel member of the human histone deacetylase family. *J. Biol. Chem.* **2002**, *277*, 25748–25755.
(12) Glaser, K. B. HDAC inhibitors: Clinical update and mechanism-based potential. *Biochem. Pharmacol.* **2007**, *74*, 659–671, and references cited therein.
(13) Garber, K. HDAC inhibitors overcome first hurdle. *Nat. Biotechnol.* **2007**, *25*, 17–19.
(14) Marks, P. A. Discovery and development of SAHA as an anticancer agent. *Oncogene* **2007**, *26*, 1351–1356.
(15) Marks, P. A.; Breslow, R. Dimethyl sulfoxide to vorinostat: development of this histone deacetylase inhibitor as an anticancer drug. *Nat. Biotechnol.* **2007**, *25*, 84–90.
(16) Bernstein, B. E.; Tong, J. K.; Schreiber, S. L. Genomewide studies of histone deacetylase function in yeast. *Proc. Natl. Acad. Sci. U.S.A.* **2000**, *97*, 13708–13713.
(17) Glaser, K. B.; Li, J.; Staver, M. J.; Wei, R. Q.; Albert, D. H.; Davidsen, S. K. Role of class I and class II histone deacetylases in carcinoma cells using siRNA. *Biochem. Biophys. Res. Commun.* **2003**, *310*, 529–536.
(18) Nielsen, T. K.; Hildmann, C.; Dickmanns, A.; Schwienhorst, A.; Ficner, R. Crystal structure of a bacterial class 2 histone deacetylase homologue. *J. Mol. Biol.* **2005**, *354*, 107–120.
(19) Vannini, A.; Volpari, C.; Filocamo, G.; Casavola, E. C.; Brunetti, M.; Renzoni, D.; Chakravarty, P.; Paolini, C.; De Francesco, R.; Gallinari, P.; Steinkèuhler, C.; Di Marco, S. Crystal structure of a eukaryotic zinc-dependent histone deacetylase, human HDAC8, complexed with a hydroxamic acid inhibitor. *Proc. Natl. Acad. Sci. U.S.A.* **2004**, *101*, 15064–15069.
(20) Somoza, J. R.; Skene, R. J.; Katz, B. A.; Mol, C.; Ho, J. D.; Jennings, A. J.; Luong, C.; Arvai, A.; Buggy, J. J.; Chi, E.; Tang, J.; Sang, B. C.; Verner, E.; Wynands, R.; Leahy, E. M.; Dougan, D. R.; Snell, G.; Navre, M.; Knuth, M. W.; Swanson, R. V.; McRee, D. E.; Tari, L. W. Structural snapshots of human HDAC8 provide insights into the class I histone deacetylases. *Structure* **2004**, *12*, 1325–1334.
(21) Sternson, S. M.; Wong, J. C.; Grozinger, C. M.; Schreiber, S. L. Synthesis of 7200 small molecules based on a substructural analysis of the histone deacetylase inhibitors trichostatin and trapoxin. *Org. Lett.* **2001**, *3*, 4239–4242.
(22) Kozikowski, A. P.; Chen, Y.; Gaysin, A.; Chen, B.; D'Annibale, M. A.; Suto, C. M.; Langley, B. C. Functional Differences in Epigenetic Modulators: Superiority of Mercaptoacetamide-Based Histone Deacetylase Inhibitors Relative to Hydroxamates in Cortical Neuron Neuroprotection Studies. *J. Med. Chem.* **2007**, *50*, 3064–3061.
(23) Kozikowski, A. P.; Chen, Y.; Gaysin, A.; Billadeau, D. D.; Kim, K., H. Chemistry, Biology, and QSAR Studies of Substituted Biaryl Hydroxamates and Mercaptoacetamides as HDAC inhibitors: Nanomolar Potency Inhibitors of Pancreatic Cancer Cell Growth. *ChemMedChem* **2008**, *3*, 487–501.
(24) Huisgen, R. *Introduction, Survey, Mechanism in 1,3-Dipolar Cycloaddition*; Padwa, A. Ed.; John Wiley & Sons: New York, 1984, *1*, 76−147.
(25) Tornøe, G. C.; Pirali, T.; Billington, R. A.; Canonico, P. L.; Sorba, G.; Genazzani, A. A. Click chemistry reactions in medicinal chemistry: Applications of the 1,3-dipolar cycloaddition between azides and alkynes. *Med. Res. Rev.* **2008**, *28*, 278–308.
(26) Rostovtsev, V. V.; Green, L. G.; Fokin, V. V.; Sharpless, K. B. A stepwise huisgen cycloaddition process: copper(I)-catalyzed regioselective "ligation" of azides and terminal alkynes. *Angew. Chem., Int. Ed.* **2002**, *41*, 2596–2599.
(27) Torn2e, C. W.; Christensen, C.; Meldal, M. Peptidotriazoles on solid phase: [1,2,3]-triazoles by regiospecific copper(I)-catalyzed 1,3-dipolar cycloadditions of terminal alkynes to azides. *J. Org. Chem.* **2002**, *67*, 3057–3064.
(28) Zhang, L.; Chen, X.; Xue, P.; Sun, H. H.; Williams, I. D.; Sharpless, K. B.; Fokin, V. V.; Jia, G. Ruthenium-catalyzed cycloaddition of alkynes and organic azides. *J. Am. Chem. Soc.* **2005**, *127*, 15998–15999.
(29) Kozikowski, A. P. The isoxazoline route to the molecules of nature. *Acc. Chem. Res.* **1984**, *17*, 410–416.
(30) Sivakumar, K.; Xie, F.; Cash, B. M.; Long, S.; Barnhill, H. N.; Wang, Q. A fluorogenic 1,3-dipolar cycloaddition reaction of 3-azidocoumarins and acetylenes. *Org. Lett.* **2004**, *6*, 4603–4606.
(31) Hubbert, C.; Guardiola, A.; Shao, R.; Kawaguchi, Y.; Ito, A.; Nixon, A.; Yoshida, M.; Wang, X. F.; Yao, T. P. HDAC6 is a microtubule-associated deacetylase. *Nature* **2002**, *417*, 455–458.
(32) Kovacs, J. J.; Murphy, P. J.; Gaillard, S.; Zhao, X.; Wu, J. T.; Nicchitta, C. V.; Yoshida, M.; Toft, D. O.; Pratt, W. B.; Yao, T. P. HDAC6 regulates Hsp90 acetylation and chaperone-dependent activation of glucocorticoid receptor. *Mol. Cell* **2005**, *18*, 601–607.

(33) Hook, S. S.; Orian, A.; Cowley, S. M.; Eisenman, R. N. Histone deacetylase 6 binds polyubiquitin through its zinc finger (PAZ domain) and copurifies with deubiquitinating enzymes. *Proc. Natl. Acad. Sci. U.S.A.* **2002**, *99*, 13425–13430.

(34) Iwata, A.; Riley, B. E.; Johnston, J. A.; Kopito, R. R. HDAC6 and microtubules are required for autophagic degradation of aggregated huntingtin. *J. Biol. Chem.* **2005**, *280*, 40282–40292.

(35) Wong, J. C.; Hong, R.; Schreiber, S. L. Structural biasing elements for in-cell histone deacetylase paralog selectivity. *J. Am. Chem. Soc.* **2003**, *125*, 5586–5587.

(36) Haggarty, S. J.; Koeller, K. M.; Wong, J. C.; Butcher, R. A.; Schreiber, S. L. Multidimensional chemical genetic analysis of diversity-oriented synthesis-derived deacetylase inhibitors using cell-based assays. *Chem. Biol.* **2003**, *10*, 383–396.

(37) Haggarty, S. J.; Koeller, K. M.; Wong, J. C.; Grozinger, C. M.; Schreiber, S. L. Domain-selective small-molecule inhibitor of histone deacetylase 6 (HDAC6)-mediated tubulin deacetylation. *Proc. Natl. Acad. Sci. U.S.A.* **2003**, *100*, 4389–4394.

(38) Suzuki, T.; Kouketsu, A.; Itoh, Y.; Hisakawa, S.; Maeda, S.; Yoshida, M.; Nakagawa, H.; Miyata, N. Highly potent and selective histone deacetylase 6 inhibitors designed based on a small-molecular substrate. *J. Med. Chem.* **2006**, *49*, 4809–4812.

(39) Itoh, Y.; Suzuki, T.; Kouketsu, A.; Suzuki, N.; Maeda, S.; Yoshida, M.; Nakagawa, H.; Miyata, N. Design, Synthesis, Structure-Selectivity Relationship, and Effect on Human Cancer Cells of a Novel Series of Histone Deacetylase 6-Selective Inhibitors. *J. Med. Chem.* **2007**, *50*, 5425–5438.

(40) Kumagai, T.; Wakimoto, N.; Yin, D.; Gery, S.; Kawamata, N.; Takai, N.; Komatsu, N.; Chumakov, A.; Imai, Y.; Koeffler, H. P. Histone deacetylase inhibitor, suberoylanilide hydroxamic acid (Vorinostat, SAHA) profoundly inhibits the growth of human pancreatic cancer cells. *Int. J. Cancer* **2007**, *121*, 656–665.

(41) Khan, N.; Jeffers, M.; Kumar, S.; Hackett, C.; Boldog, F.; Khramtsov, N.; Qian, X.; Mills, E.; Berghs, S. C.; Carey, N.; Finn, P. W.; Collins, L. S.; Tumber, A.; Ritchie, J. W.; Jensen, P. B.; Lichenstein, H. S.; Sehested, M. Determination of the class and isoform selectivity of small molecule HDAC inhibitors. *Biochem. J.* **2007**, *409*, 581–589.

(42) Sato, N.; Ohta, T.; Kitagawa, H.; Kayahara, M.; Ninomiya, I.; Fushida, S.; Fujimura, T.; Nishimura, G.; Shimizu, K.; Miwa, K. FR901228, a novel histone deacetylase inhibitor, induces cell cycle arrest and subsequent apoptosis in refractory human pancreatic cancer cells. *Int. J. Oncol.* **2004**, *24*, 679–685.

(43) Curtin, M.; Glaser, K. Histone deacetylase inhibitors: the Abbott experience. *Curr. Med. Chem.* **2003**, *10*, 2373–2392.

(44) Morrison, B. E.; Majdzadeh, N.; Zhang, X.; Lyles, A.; Bassel-Duby, R.; Olson, E. N.; D'Mello, S. R. Neuroprotection by histone deacetylase-related protein. *Mol. Biol. Cell* **2006**, *26*, 3550–3564.

(45) World Health Organization *World Malaria Report 2005*; World Health Organization: Geneva, 2005; http://www.rbm.who.int/wmr2005/.

(46) Darkin-Rattray, S. J.; Gurnett, A. M.; Myers, R. W.; Dulski, P. M.; Crumley, T. M.; Allocco, J. J.; Cannova, C.; Meinke, P. T.; Colletti, S. L.; Bednarek, M. A.; Singh, S. B.; Goetz, M. A.; Dombrowski, A. W.; Polishook, J. D.; Schmatz, D. M. Apicidin: a novel antiprotozoal agent that inhibits parasite histone deacetylase. *Proc. Natl. Acad. Sci. U.S.A.* **1996**, *93*, 13143–13147.

(47) Joshi, M. B.; Lin, D. T.; Chiang, P. H.; Goldman, N. D.; Fujioka, H.; Aikawa, M.; Syin, C. Molecular cloning and nuclear localization of a histone deacetylase homologue in Plasmodium falciparum. *Mol. Biochem. Parasitol.* **1999**, *99*, 11–19.

(48) Andrews, K. T.; Walduck, A.; Kelso, M. J.; Fairlie, D. P.; Saul, A.; Parsons, P. G. Anti-malarial effect of histone deacetylation inhibitors and mammalian tumour cytodifferentiating agents. *Int. J. Parasitol.* **2000**, *30*, 761–768.

(49) Desjardins, R. E.; Canfield, C. J.; Haynes, J. D.; Chulay, J. D. Quantitative assessment of antimalarial activity in vitro by a semiautomated microdilution technique. *Antimicrob. Agents Chemother.* **1979**, *16*, 710–718.

(50) Milhous, W. K.; Weatherly, N. F.; Bowdre, J. H.; Desjardins, R. E. In vitro activities of and mechanisms of resistance to antifol antimalarial drugs. *Antimicrob. Agents Chemother.* **1985**, *27*, 525–530.

(51) Dow, G. S.; Koenig, M. L.; Wolf, L.; Gerena, L.; Lopez-Sanchez, M.; Hudson, T. H.; Bhattacharjee, A. K. The antimalarial potential of 4-quinolinecarbinolamines may be limited due to neurotoxicity and cross-resistance in mefloquine-resistant Plasmodium falciparum strains. *Antimicrob. Agents Chemother.* **2004**, *48*, 2624–2632.

JM701606B